

A FULLY ALGEBRAIC AND ROBUST TWO-LEVEL SCHWARZ METHOD BASED ON OPTIMAL LOCAL APPROXIMATION SPACES

ALEXANDER HEINLEIN AND KATHRIN SMETANA

ABSTRACT. Two-level domain decomposition preconditioners lead to fast convergence and scalability of iterative solvers. However, for highly heterogeneous problems, where the coefficient function is varying rapidly on several possibly non-separated scales, the condition number of the preconditioned system generally depends on the contrast of the coefficient function leading to a deterioration of convergence. Enhancing the methods by coarse spaces constructed from suitable local eigenvalue problems, also denoted as adaptive or spectral coarse spaces, restores robust, contrast-independent convergence. However, these eigenvalue problems typically rely on non-algebraic information, such that the adaptive coarse spaces cannot be constructed from the fully assembled system matrix.

In this paper, a novel algebraic adaptive coarse space, which relies on the a -orthogonal decomposition of (local) finite element (FE) spaces into functions that solve the partial differential equation (PDE) with some trace and FE functions that are zero on the boundary, is proposed. In particular, the basis is constructed from eigenmodes of two types of local eigenvalue problems associated with the edges of the domain decomposition. To approximate functions that solve the PDE locally, we employ a transfer eigenvalue problem, which has originally been proposed for the construction of optimal local approximation spaces for multiscale methods. In addition, we make use of a Dirichlet eigenvalue problem that is a slight modification of the Neumann eigenvalue problem used in the adaptive generalized Dryja–Smith–Widlund (AGDSW) coarse space. Both eigenvalue problems rely solely on local Dirichlet matrices, which can be extracted from the fully assembled system matrix. By combining arguments from multiscale and domain decomposition methods we derive a contrast-independent upper bound for the condition number.

The robustness of the method is confirmed numerically for a variety of heterogeneous coefficient distributions, including binary random distributions and a coefficient function constructed from the SPE10 benchmark. The results are comparable to those of the non-algebraic AGDSW coarse space, also for those cases where the convergence of the classical algebraic generalized Dryja–Smith–Widlund (GDSW) coarse space deteriorates. Moreover, the coarse space dimension is the same or comparable to the AGDSW coarse space for all numerical experiments.

1. INTRODUCTION

Domain decomposition methods (DDMs) are a popular class of methods that yield rapid convergence in the iterative solution of linear systems of equations arising from partial differential equations (PDEs). In particular, if a suitable coarse level is used, DDMs have proved to be scalable for a wide range of problems, which, for elliptic problems, can be shown theoretically by proving an upper bound for the condition number.

Unfortunately, in presence of strong heterogeneities in certain problem parameters, the convergence of classical DDMs may deteriorate. For instance, for a diffusion problem with a coefficient function that is varying rapidly on possibly several non-separated scales, the condition number may depend on the contrast of the maximum and minimum values of the

Date: July 13, 2022.

2010 Mathematics Subject Classification. 65F08, 65F10, 65N55, 65N30, 68W10.

Key words and phrases. Domain decomposition methods, multiscale methods, overlapping Schwarz preconditioner, adaptive coarse spaces.

coefficient. One way to overcome this issue is by using adaptive coarse spaces, also known as spectral coarse spaces. These approaches are based on solving local generalized eigenvalue problems and selecting a number of eigenfunctions based on a user-chosen tolerance for the eigenvalues. The selected functions are used to construct coarse basis functions with local support. Due to the use of spectral information, these coarse spaces typically yield a provable upper bound of the condition number that is independent of the contrast and depends on the tolerance for the eigenvalues. Hence, adaptive coarse spaces yield robust convergence. A variety of adaptive coarse spaces has been introduced for nonoverlapping DDMs [44, 59, 37, 36, 61, 7, 45, 10, 35, 49], most of which consider finite element tearing and interconnect – dual primal (FETI–DP) and balancing domain decomposition by constraints (BDDC) methods, and overlapping Schwarz methods [19, 18, 15, 58, 28, 27, 29, 30, 17, 20, 39, 6].

Even though provably robust, none of the approaches referenced above is algebraic. This means that none of the above-mentioned preconditioners can be constructed from the fully assembled system matrix therefore requiring new assembly routines and potentially even access to the mesh of the FE discretization. FETI-DP and BDDC methods are generally not algebraic since they require local Neumann matrices on the subdomains, which cannot be extracted from the system matrix. Schwarz methods can be constructed algebraically if the coarse space can be constructed algebraically. However, the adaptive coarse spaces mentioned above all require additional information for the definition of the eigenvalue problems, such as local Neumann matrices or geometric information.

In this paper, we propose, to the best of our knowledge for the first time, an interface-based adaptive coarse space for two-level overlapping Schwarz methods that is both fully algebraic and robust. Relying on the well-known a -orthogonal decomposition of local FE spaces into functions that solve the PDE numerically with a prescribed trace as a boundary condition and FE functions that are zero on the boundary, we propose in this paper building the adaptive coarse space from two local eigenvalue problems associated with each edge of the domain decomposition. To approximate functions that solve the PDE locally, we employ the transfer eigenvalue problem introduced in [55], which is known from the construction of optimal local approximation spaces [5, 55, 42, 53] for a novel type of multiscale methods that allows full error control even for heterogeneous problems with non-separated scales [5, 43, 42, 47, 48, 46, 55]. For the approximation of the functions with zero trace we make use of a Dirichlet eigenvalue problem which is a slight modification of the Neumann eigenvalue problem used in the non-algebraic adaptive generalized Dryja–Smith–Widlund (AGDSW) [27, 29, 30, 39] coarse space. The adaptive coarse space is then build from energy-minimizing extensions of the eigenfunctions. Our new method is algebraic as both eigenvalue problems rely solely on local Dirichlet matrices, which can be extracted from the fully assembled system matrix. We show that using and combining arguments from these novel type of multiscale methods and DDMs allows deriving a contrast-independent upper bound for the condition number.

In [41, 40], techniques from Schwarz methods have been used to develop and analyze such novel type of multiscale methods, highlighting a connection between the latter and certain DDMs.

The adaptive coarse space proposed in this paper belongs to a class of adaptive coarse spaces which first partition the interface into nonoverlapping components and compute the eigenvalue problems on these components; cf. the spectral harmonically enriched multiscale (SHEM) [20, 17], overlapping Schwarz – approximate component synthesis (OS-ACMS) [28], and AGDSW coarse spaces. All these approaches yield a minimum number of total degrees of freedom in all local generalized eigenvalue problems since no degree of freedom appears in more than one eigenvalue problem. Our new method is most closely related to the AGDSW

method. Even though the AGDSW coarse space contains the generalized Dryja–Smith–Widlund (GDSW) coarse space [13, 14], which can be constructed algebraically, it is not algebraic since local Neumann matrices appear in the eigenvalue problems.

Algebraic coarse spaces for overlapping Schwarz methods have recently, and in parallel to the preparation of this manuscript, also been proposed by Gouarin and Spillane [23, 57] as well as Al Daas et al. [2, 3, 4]. In both cases, the methods can be seen as extensions of the generalized eigenproblems in the overlaps (GenEO) [58] approach, where local eigenvalue problems in the overlaps or the overlapping subdomains of the Schwarz method are solved to compute the coarse space. In order to obtain algebraic coarse spaces, the authors mostly focus on general linear algebra arguments, such as matrix splittings and the Sherman–Morrison–Woodbury formula; see also [56, 1] for abstract descriptions of the GenEO framework. In contrast, our approach is based on a priori knowledge about the elliptic PDE. We conjecture that the proposed methodology can be readily extended to other elliptic problems such as linear elasticity, parabolic problems, and higher spatial dimensions; see also the extensions of the related AGDSW method [29, 30].

Note that algebraic multigrid (AMG) methods [52] are another famous class of algebraic solvers for linear systems of equations, and spectral information has also been used to improve their robustness, for instance, in the spectral element-based algebraic multigrid (ρ AMG) method [11].

The paper is organized as follows: We propose adaptive coarse spaces for DDMs that are fully algebraic in section 5 and derive a bound for the condition number in section 6. Beforehand, we briefly introduce our heterogeneous diffusion model problem in section 2 and review two-level overlapping Schwarz preconditioner in subsection 3.1 and adaptive coarse spaces in subsection 3.2. In particular, we also elaborate in section 4 on the challenges that arise when one wishes to construct adaptive coarse spaces without relying on local discrete variational problems with Neumann boundary conditions that would require new assembly routines on the local subdomains. Finally, we discuss the computational realization of the proposed method in section 7 and demonstrate its robustness numerically in section 8.

2. PROBLEM SETTING

Let $\Omega \subset \mathbb{R}^2$ be a bounded domain with Lipschitz boundary and $\alpha \in L^\infty(\Omega)$ with $0 < \alpha_{min} \leq \alpha \leq \alpha_{max} < \infty$ be a highly heterogeneous coefficient function, possibly with high jumps. We consider the variational problem:

$$(1) \quad \text{Find } u \in H_0^1(\Omega) : \quad a_\Omega(u, v) = f(v) \quad \forall v \in H_0^1(\Omega),$$

$$\text{where } a_\Omega(u, v) := \int_\Omega \alpha(x) (\nabla u(x))^T \nabla v(x) dx \quad \text{and} \quad f(v) := \int_\Omega f(x) v(x) dx,$$

respectively, and $f \in L^2(\Omega)$. We equip $H_0^1(\Omega)$ with the energy norm $|u|_{a_\Omega} := (a_\Omega(u, u))^{1/2}$. Due to space limitations, we defer a discussion of the treatment of Neumann or mixed boundary conditions to a forthcoming paper.

Let τ_h be a quasi-uniform triangulation of Ω into triangles or quadrilaterals with element size h . To simplify the presentation, we assume that the triangulation resolves the coefficient function, i.e., that α is constant on each element. Then, we introduce a conforming finite element (FE) space $V_\Omega^0 \subset H_0^1(\Omega)$ of dimension N_Ω , where, for the sake of simplicity, we consider piece-wise linear (P1) or bilinear (Q1) FE spaces. We obtain the following discrete variational problem:

$$(2) \quad \text{Find } u \in V_\Omega^0 : \quad a_\Omega(u, v) = f(v) \quad \forall v \in V_\Omega^0,$$

where $f(v) := \int_{\Omega} f(x)v(x) dx$ for $v \in V_{\Omega}^0$. The algebraic version of (2) then reads

$$(3) \quad \text{Find } \mathbf{u} \in \mathbb{R}^{N_{\Omega}} : \mathbf{A}\mathbf{u} = \mathbf{f}, \quad \text{where } \mathbf{A} \in \mathbb{R}^{N_{\Omega} \times N_{\Omega}}, \mathbf{f} \in \mathbb{R}^{N_{\Omega}}.$$

3. ADAPTIVE COARSE SPACES FOR TWO-LEVEL OVERLAPPING SCHWARZ PRECONDITIONERS

3.1. Two-Level Overlapping Schwarz Preconditioner. Let Ω be decomposed into nonoverlapping subdomains Ω_i with maximal diameter H such that $\bar{\Omega} = \bigcup_{i=1}^M \bar{\Omega}_i$, $\Omega_i \cap \Omega_j = \emptyset$ for $i \neq j$. We assume that the boundaries of the subdomains are Lipschitz continuous and do not intersect any element of τ_h . The domain decomposition interface is given as

$$(4) \quad \Gamma = \bigcup_{i \neq j} (\partial\Omega_i \cap \partial\Omega_j) \setminus \partial\Omega.$$

Let then $\{\Omega'_i\}_{i=1}^M$ be a corresponding overlapping decomposition of Ω with overlap $\delta \geq h$. We introduce associated conforming FE spaces $V_{\Omega'_i}^0 \subset H_0^1(\Omega'_i)$, $i = 1, \dots, M$, and introduce operators $R_{\Omega \rightarrow \Omega'_i} : V_{\Omega}^0 \rightarrow V_{\Omega'_i}^0$ that *restrict* FE functions in V_{Ω}^0 to $V_{\Omega'_i}^0$. The operators $E_{\Omega'_i \rightarrow \Omega} : V_{\Omega'_i}^0 \rightarrow V_{\Omega}^0$ *extend* FE functions in $V_{\Omega'_i}^0$ by zero to FE functions in V_{Ω}^0 accordingly. Note that the indices of the restriction and extension operators $R_{\Omega \rightarrow \Omega'_i}$ and $E_{\Omega'_i \rightarrow \Omega}$ here and henceforth show the domain of the respective FE spaces the operators map from and to.¹

Next, we introduce local bilinear forms $a_{\Omega'_i} : V_{\Omega'_i}^0 \times V_{\Omega'_i}^0 \rightarrow \mathbb{R}$ and corresponding local stiffness matrices $\mathbf{A}_{\Omega'_i}$, $i = 1, \dots, M$. We use exact local solvers and thus obtain

$$(5) \quad a_{\Omega'_i}(u_i, v_i) = a_{\Omega}(E_{\Omega'_i \rightarrow \Omega}u_i, E_{\Omega'_i \rightarrow \Omega}v_i) \quad \forall u_i, v_i \in V_{\Omega'_i}^0, \quad \mathbf{A}_{\Omega'_i} = \mathbf{R}_{\Omega \rightarrow \Omega'_i} \mathbf{A} \mathbf{E}_{\Omega'_i \rightarrow \Omega},$$

for $i = 1, \dots, M$, where $\mathbf{R}_{\Omega \rightarrow \Omega'_i}$ and $\mathbf{E}_{\Omega'_i \rightarrow \Omega} = \mathbf{R}_{\Omega \rightarrow \Omega'_i}^T$ are the algebraic counterparts of $R_{\Omega \rightarrow \Omega'_i}$ and $E_{\Omega'_i \rightarrow \Omega}$, respectively; cf. [60]. Following, e.g., [60, 51] we introduce operators $\tilde{P}_i : V_{\Omega}^0 \rightarrow V_{\Omega'_i}^0$, defined as

$$(6) \quad a_{\Omega'_i}(\tilde{P}_i u, v_i) = a_{\Omega}(u, E_{\Omega'_i \rightarrow \Omega}v_i), \quad \text{for } v_i \in V_{\Omega'_i}^0, \quad i = 1, \dots, M.$$

We may then define projections

$$(7) \quad P_i = E_{\Omega'_i \rightarrow \Omega} \tilde{P}_i : V_{\Omega}^0 \rightarrow E_{\Omega'_i \rightarrow \Omega} V_{\Omega'_i}^0 \subset V_{\Omega}^0, \quad i = 1, \dots, M,$$

with algebraic counterparts $\mathbf{P}_i = \mathbf{E}_{\Omega'_i \rightarrow \Omega} \mathbf{A}_{\Omega'_i}^{-1} \mathbf{R}_{\Omega \rightarrow \Omega'_i} \mathbf{A}$, $i = 1, \dots, M$; see [60]. The additive Schwarz operator $P_{AS-1} := \sum_{i=1}^M P_i$ then reads in matrix form as

$$(8) \quad \mathbf{P}_{AS-1} := \sum_{i=1}^M \mathbf{E}_{\Omega'_i \rightarrow \Omega} \mathbf{A}_{\Omega'_i}^{-1} \mathbf{R}_{\Omega \rightarrow \Omega'_i} \mathbf{A} = \sum_{i=1}^M \mathbf{R}_{\Omega \rightarrow \Omega'_i}^T \mathbf{A}_{\Omega'_i}^{-1} \mathbf{R}_{\Omega \rightarrow \Omega'_i} \mathbf{A}.$$

This Schwarz operator is a preconditioned operator $\mathbf{M}_{AS-1}^{-1} \mathbf{A}$ consisting of the one-level Schwarz preconditioner $\mathbf{M}_{AS-1}^{-1} = \sum_{i=1}^M \mathbf{E}_{\Omega'_i \rightarrow \Omega} \mathbf{A}_{\Omega'_i}^{-1} \mathbf{R}_{\Omega \rightarrow \Omega'_i}$ and the system matrix \mathbf{A} . In this one-level Schwarz method, information is only exchanged between neighboring subdomains through the overlaps, and as a result, the convergence generally deteriorates for a large number of subdomains; see [51]. As a remedy, one may add a global coarse space $X_0 \subset V_{\Omega}^0$.² Correspondingly, we introduce an interpolation operator $E_0 : X_0 \rightarrow V_{\Omega}^0$, which expresses

¹Very often the operators $R_{\Omega \rightarrow \Omega'_i}$ and $E_{\Omega'_i \rightarrow \Omega}$ are denoted by R_i and R_i^T in the literature; see, e.g., [60]). As we will be needing also additional restriction and extension operators e.g., for FE spaces on the edges or Γ , we indicate the domains of the associated FE spaces here.

²In many publications, the coarse space is denoted by V_0 . However, to avoid confusion with FE spaces including functions with zero trace, we denote the coarse space here by X_0 .

functions in X_0 in the FE-basis of V_Ω^0 . The columns of the algebraic counterpart \mathbf{E}_0 therefore contain the FE coefficients of the basis functions of X_0 . Introducing the corresponding restriction operator $R_0 : V_\Omega^0 \rightarrow X_0$ and its algebraic counterpart $\mathbf{R}_0 = \mathbf{E}_0^T$, we can define $P_0 = E_0 \tilde{P}_0 : V_\Omega^0 \rightarrow E_0 X_0 \subset V_\Omega^0$. We define the operator \tilde{P}_0 analogously to (6), where

$$(9) \quad a_0(u_0, v_0) = a_\Omega(E_0 u_0, E_0 v_0) \quad \forall u_0, v_0 \in X_0, \quad \mathbf{A}_0 = \mathbf{R}_0 \mathbf{A} \mathbf{E}_0 = \mathbf{R}_0 \mathbf{A} \mathbf{R}_0^T;$$

this means that we also consider the case of an exact coarse solver. We then define the two-level Schwarz operator [60] $P_{AS-2} := \sum_{i=1}^M P_i$, and its algebraic counterpart takes the form

$$(10) \quad \mathbf{P}_{AS-2} = \mathbf{M}_{AS-2}^{-1} \mathbf{A} := \underbrace{\mathbf{E}_0 \mathbf{A}_0^{-1} \mathbf{R}_0 \mathbf{A}}_{\text{coarse level}} + \underbrace{\sum_{i=1}^M \mathbf{E}_{\Omega'_i \rightarrow \Omega} \mathbf{A}_{\Omega'_i}^{-1} \mathbf{R}_{\Omega \rightarrow \Omega'_i} \mathbf{A}}_{\text{first level}}.$$

Different choices of coarse spaces X_0 yield numerically scalable preconditioners, that is, a condition number bound which is independent of the number of subdomains. As a result, the convergence of iterative solvers, such as Krylov subspace methods, with such a two-level Schwarz preconditioner is independent of the number of subdomains as well. However, using a standard Lagrangian FE basis, for X_0 , we obtain the condition number bound

$$(11) \quad \kappa(\mathbf{P}_{AS-2}) = \kappa(\mathbf{M}_{AS-2}^{-1} \mathbf{A}) \leq C \max_{T \in \tau_H} \max_{x, y \in \omega_T} \left(\frac{\alpha(x)}{\alpha(y)} \right) \left(1 + \frac{H}{\delta} \right)$$

for our model problem (1); similar bounds hold for other classical (non-adaptive) coarse spaces. Here, τ_H is the coarse triangulation, which, in our case, coincides with the nonoverlapping domain decomposition $\{\Omega_i\}_{i=1, \dots, N}$. Moreover, ω_T corresponds to the union of all coarse mesh elements which touch a coarse mesh element T . Sharper variants of this estimate can be derived, but the dependence on the contrast of the coefficient function remains; see [24]. This means that the convergence of a Krylov subspace method preconditioned with this two-level Schwarz preconditioner might actually depend on the contrast of the coefficient function α , resulting in very high iteration counts; cf. also the results in section 8.

3.2. Adaptive Coarse Spaces. Figure 1 attempts to visualize one of the reasons that the coefficient contrast may arise in the condition number bound. The energy

$$(12) \quad |\cdot|_{a, \Omega}^2 := a_\Omega(\cdot, \cdot)$$

of the function u plotted in Fig. 1 (left) depends only on the minimum value α_{\min} of the coefficient function α but is independent of the maximum value α_{\max} as its gradient is zero (green) in the yellow region, where $\alpha = \alpha_{\max}$. If we interpolate the function with piecewise bilinear Lagrangian basis functions (see Fig. 1 (right)) the interpolant u_0 decays to zero within the yellow region (red), and hence, its energy clearly depends on α_{\max} . Therefore, in any energy estimate of the coarse interpolation, which is part of the proof of a condition number bound in the abstract Schwarz theory [60],

$$(13) \quad |u_0|_{a, \Omega}^2 \leq C |u|_{a, \Omega}^2,$$

the constant C has to depend on the contrast of α , $\alpha_{\max}/\alpha_{\min}$. Therefore, in order to obtain a robust condition number bound, the coefficient function has to be taken into account in the construction of the coarse space; as we will also observe in section 8, it is additionally necessary to add one coarse basis function for each high coefficient component crossing the domain decomposition interface.

Adaptive coarse spaces account for variations in the coefficient functions by including eigenfunctions of local eigenvalue problems into the coarse space, which is why they are also denoted as *spectral coarse spaces*. The term *adaptive* stems from the fact that all eigenvalues

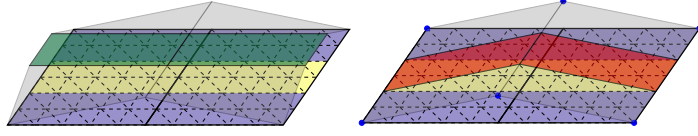


FIGURE 1. For a heterogeneous coefficient function, a Lagrangian coarse interpolation (here, piecewise bilinear; right) of a low-energy function (left) may have a high energy: Let the yellow part of the two (nonoverlapping) subdomains correspond to a high coefficient (α_{\max}) and the blue part to a low coefficient (α_{\min}). Since the function itself is constant (marked in green) in the high coefficient region but varying in the remaining part, the energy depends on α_{\min} but not on α_{\max} . The piecewise linear interpolation has a nonzero gradient everywhere, such that the energy depends on α_{\max} (marked in red). In this case, the stability constant of the interpolation depends on the contrast of the coefficient function.

below a certain tolerance tol can be included in the coarse space, resulting in a condition number bound of the form

$$(14) \quad \kappa(\mathbf{P}_{AS-2}) = \kappa(\mathbf{M}_{AS-2}^{-1}\mathbf{A}) \leq C \left(1 + \frac{1}{tol}\right),$$

where C is independent of the contrast of the coefficient function. Hence, the number of coarse basis functions does not have to be determined beforehand, but it is chosen adaptively based on tol .

In this paper, we develop a new energy-minimizing adaptive coarse space consisting of basis functions which minimize the energy $|\cdot|_{a,\Omega_i}^2$ on each nonoverlapping subdomain. Energy-minimizing functions are part of constructing a coarse space with a contrast-independent energy (13). Moreover, constructing the coarse basis by energy-minimization is one of the key ingredients for algebraicity since it does not require the availability of a coarse triangulation. In particular, the energy-minimizing extension $v_i = H_{\partial\Omega_i \rightarrow \Omega_i}(v_{\partial\Omega_i})$ from $\partial\Omega_i$ to Ω_i for a FE function $v_{\partial\Omega_i}$ on $\partial\Omega_i$ is defined as follows: given some boundary values $v_{\partial\Omega_i}$ on the interface, the corresponding extension $H_{\partial\Omega_i \rightarrow \Omega_i}(v_{\partial\Omega_i})$ solves

$$(15) \quad v_i = \arg \min_{v|_{\partial\Omega_i} = v_{\partial\Omega_i}} |v|_{a,\Omega_i}^2 \Leftrightarrow \begin{cases} a_{\Omega_i}(v_i, w_i) = 0 & \forall w_i \in V_{\Omega_i}^0, \\ v_i = v_{\partial\Omega_i} & \text{on } \partial\Omega_i. \end{cases}$$

An energy-minimizing extension $v = H_{\Gamma \rightarrow \Omega}(v_{\Gamma})$ extends interface values v_{Γ} into the interior of each subdomain, with zero Dirichlet boundary conditions on $\partial\Omega$. In matrix form, this corresponds to

$$(16) \quad \mathbf{v} = \begin{pmatrix} -\mathbf{A}_{II}^{-1}\mathbf{A}_{I\Gamma} \\ \mathbf{I}_{\Gamma} \end{pmatrix} \mathbf{v}_{\Gamma},$$

where we make use of the splitting of the rows and columns corresponding to interior (I) and interface (Γ) nodes

$$\mathbf{A} = \begin{pmatrix} \mathbf{A}_{II} & \mathbf{A}_{I\Gamma} \\ \mathbf{A}_{\Gamma I} & \mathbf{A}_{\Gamma\Gamma} \end{pmatrix}$$

and \mathbf{I}_{Γ} corresponds to the identity matrix on the degrees of freedom of Γ . Here, as usual, the Dirichlet boundary degrees of freedom are counted as interior degrees of freedom. Due to the Dirichlet boundary conditions in \mathbf{A} , the boundary conditions are then enforced automatically. Note that $\mathbf{A}_{II} = \text{diag}(\mathbf{A}_{\Omega_i,II})$ is a block-diagonal matrix, where $\mathbf{A}_{\Omega_i,II}$ is the matrix corresponding to the interior degrees of freedom in Ω_i . Hence, in a parallel setting, \mathbf{A}_{II}^{-1} can be applied independently and concurrently for the subdomains. Moreover, we have that $|v|_{a,\Omega_i}^2 = a_{\Omega_i}(v, v) = \mathbf{v}^T \mathbf{A} \mathbf{v} = \mathbf{v}_{\Gamma}^T \mathbf{S} \mathbf{v}_{\Gamma}$, with the Schur complement $\mathbf{S} = \mathbf{A}_{\Gamma\Gamma} - \mathbf{A}_{\Gamma I} \mathbf{A}_{II}^{-1} \mathbf{A}_{I\Gamma}$.

Let us now discuss the general idea of adaptive coarse spaces which are based on an interface partition. To that end, let the interface Γ be partitioned into edges and vertices. We then solve a generalized eigenvalue problem of the form

$$(17) \quad \text{Find } \mathbf{v} \in \mathbb{R}^{N_e} \text{ such that } \mathbf{S}_e \mathbf{v} = \mu \mathbf{A}_{\tilde{e}\tilde{e}} \mathbf{v}$$

for each edge e , where N_e is the number of degrees of freedom of the interior of the edge e . Here, \mathbf{S}_e is a Schur complement corresponding to the two subdomains Ω_i and Ω_j adjacent to e , and $\mathbf{A}_{\tilde{e}\tilde{e}}$ is the restriction of the global matrix \mathbf{A} to the degrees of freedom on the interior of the edge. As mentioned above, Schur complement matrices correspond to energy-minimizing extensions. In this eigenvalue problem, we consider such an extension from the e into the adjacent subdomains. The specific definition of \mathbf{S}_e may vary slightly for different interface-based adaptive coarse spaces, such as in the boundary conditions in the endpoints of the edge e . Moreover, $\mathbf{A}_{\tilde{e}\tilde{e}}$ can also be replaced by a scaled mass matrix or a lumped version of that.

To construct an adaptive coarse space, the eigenfunctions corresponding to eigenvalues below a user-chosen tolerance tol are selected and extended by zero onto the remaining interface. Then, these functions are extended in an energy minimizing way by $H_{\Gamma \rightarrow \Omega}$, resulting in the coarse basis functions.

As will also be discussed in section 4 and visualized in Fig. 2, eigenvalue problem (17) relates a low-energy extension (\mathbf{S}_e) and a high-energy extension ($\mathbf{A}_{\tilde{e}\tilde{e}}$). Therefore, the resulting coarse basis functions corresponding to low eigenvalues capture the critical components of the coefficient function, resulting in a condition number bound of the form (14), which is independent of the contrast of the coefficient function; see, e.g., [28, 29, 30, 20].

4. MOTIVATION: CHALLENGES AND ADVANTAGES OF ROBUST ALGEBRAIC PRECONDITIONERS AND KEY NEW IDEAS

Despite the rapid development in adaptive coarse spaces, the development of algebraic adaptive coarse spaces, that is, adaptive coarse spaces that can be constructed based on the fully assembled system matrix \mathbf{A} , has been an open question for a longer time. For the practical applicability of a solver, this is, however, a desirable property. In particular, if the solver is fully algebraic, it can be used in any FE implementation which provides the linear system of equations (3) as the solver input.

Let us briefly discuss the main challenge, which can be understood in a similar way as in Fig. 1. The left- and right-hand sides of the eigenvalue problem (17) correspond to energies of certain extensions of the edge values into the interior of the adjacent subdomains. In the top left of Fig. 2, we see some function u with an energy $|u|_{a,\Omega}^2$ that does not depend on α_{\max} ; the gradient in the yellow region is zero (green). In addition three different extensions of the edge values of this function are depicted: The extension on the top right is the extension by zero, and the corresponding energy clearly depends on α_{\max} (red). The matrix in the right-hand side of (17) corresponds to this extension, that is, if $\mathbf{u}_{\tilde{e}}$ is the discrete vector with the interior edge values of u , then $\mathbf{u}_{\tilde{e}}^T \mathbf{A}_{\tilde{e}\tilde{e}} \mathbf{u}_{\tilde{e}}$ is the energy of the extension by zero (top right in Fig. 2). This extension is algebraic since the matrix can be extracted from \mathbf{A} . The extension on the bottom right is the energy-minimizing extension of u_e with Neumann data on the boundary; of all functions with trace u_e , this function has the minimum energy, which is clearly smaller or equal to the energy of u . Hence, the function satisfies an energy estimate of the form (13) with a constant C which does not depend on the contrast of α , $\frac{\alpha_{\max}}{\alpha_{\min}}$. This is precisely the extension employed in \mathbf{S}_e in the left-hand side of (17).

Unfortunately, since this extension has Neumann boundary data, the corresponding matrix \mathbf{S}_e cannot be extracted algebraically from \mathbf{A} . An algebraic alternative to this extension would be the energy-minimizing extension with Dirichlet boundary data; cf. Fig. 2 (bottom left). The Dirichlet submatrix corresponding to both subdomains adjacent to the edge e , which is

required to compute this extension, can also be extracted from \mathbf{A} . However, the energy of this extension clearly depends on α_{\max} . Hence, using this algebraic extension in (17), would also result in a dependency on $\frac{\alpha_{\max}}{\alpha_{\min}}$.

This short discussion explains why the Neumann matrix in (17) cannot be simply replaced by a Dirichlet matrix; this has also been discussed in [28]. It can be observed that, except for very recent approaches targeting algebraic adaptive coarse spaces, all early adaptive coarse spaces are based on eigenvalue problems which use Neumann matrices or information about the coefficient function and geometric information. Note that there have also been attempts to heuristically construct algebraic robust coarse spaces; cf., e.g. [28, 25, 31]. However, no theory has been proved for these approaches yet, and they might not be robust for arbitrary coefficient functions.

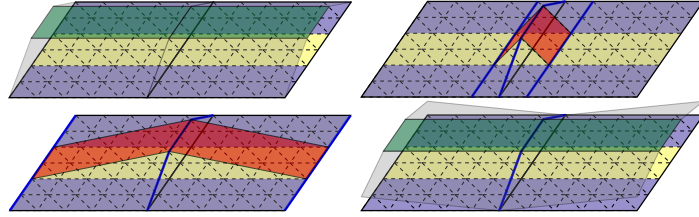


FIGURE 2. For the same configuration as in Fig. 1, we consider three different extensions of the edge values of a function (top, left): the zero extension $E_{e \rightarrow \Omega_e}$ (top, right), the harmonic extension with Dirichlet boundary data $H_{e \rightarrow \Omega_e}^{\partial \Omega_e}$ (bottom, left), and an harmonic extension with Neumann boundary data $H_{e \rightarrow \Omega_e}$ (bottom, right). The Dirichlet data of the extensions is marked in blue. Note that, in general, only the extension with Neumann boundary data has a guaranteed lower (or equal) energy compared to the original function; the energy of the other functions may even depend on the contrast.

5. A FULLY ALGEBRAIC AND ROBUST ADAPTIVE COARSE SPACE BASED ON OPTIMAL LOCAL APPROXIMATION SPACES

In this section, we propose, to the best of our knowledge for the first time, a fully algebraic and robust adaptive interface-based coarse space. To that end, we start with the vertex space and the edge space containing the constant function and enhance it by edge eigenfunctions of the *Dirichlet eigenvalue problem* introduced in subsection 5.1 and the *Transfer eigenvalue problem* introduced in subsection 5.2. As we only use Dirichlet matrices in the eigenvalue problems to obtain an algebraic method, we might miss the constant function in the edge space. However, it is well known in DDMs that a scalable coarse has to be able to represent the null space of the global Neumann operator on each subdomain which does not touch the global Dirichlet boundary. We thus start with

$$(18) \quad X_{vert} = \text{span}\{H_{\Gamma \rightarrow \Omega}(E_{\mathcal{V} \rightarrow \Gamma}(1)) : \mathcal{V} \text{ vertex}\}, \quad \text{and}$$

$$(19) \quad X_{const} = \text{span}\{H_{\Gamma \rightarrow \Omega}(E_{e \rightarrow \Gamma}(1)) : e \text{ edge}\},$$

where we consider the vertices and edges of the nonoverlapping domain decomposition $\{\Omega_i\}_{i=1, \dots, N}$. Here, $E_{\mathcal{V} \rightarrow \Gamma} : V_{\mathcal{V}} \rightarrow V_{\Gamma}^0$ and $E_{e \rightarrow \Gamma} : V_e^0 \rightarrow V_{\Gamma}^0$ extend the FE function by zero from the vertex \mathcal{V} or the edge e to the interface Γ , respectively.

Note that $X_{\text{GDSW}} = X_{vert} \oplus X_{const}$ corresponds to the classical GDSW coarse space. This space is also automatically included in the AGDSW adaptive coarse space. In particular, the constant edge function corresponds to the zero eigenvalue in the AGDSW edge eigenvalue problem due to full Neumann boundary data; hence, the function is always selected as a basis function.

5.1. A Dirichlet eigenvalue problem for the edges. As motivated in section 4, for each edge $e \in \Gamma$, we consider a Dirichlet eigenvalue problem which is a slight modification of the Neumann eigenvalue problem (17) used in the AGDSW coarse spaces; cf. [27, 29, 30]. First,

we introduce for a fixed but arbitrary edge e a so-called oversampling domain Ω_e such that $\text{dist}(\partial\Omega_e, e) \geq v_e > 0$; see Figs. 3 and 5 for illustrations of oversampling domains. In addition, we introduce $E_{e \rightarrow \Omega_e} : V_e^0 \rightarrow V_{\Omega_e}^0$, which assigns the coefficients of the FE functions on the edge e to the FE basis functions in Ω_e whose associated nodes lie on e and extends by zero on all other nodes in Ω_e ; see Fig. 2 (top right) and Fig. 5 (third column) for illustrations.

We may then introduce the corresponding inner product $b_e : V_e^0 \times V_e^0 \rightarrow \mathbb{R}$ defined

$$(20) \quad b_e(\chi, \zeta) := a_{\Omega_e}(E_{e \rightarrow \Omega_e} \chi, E_{e \rightarrow \Omega_e} \zeta) \quad \forall \chi, \zeta \in V_e^0.$$

Furthermore, we introduce the inner product $d_e : V_e^0 \times V_e^0 \rightarrow \mathbb{R}$ defined as

$$(21) \quad d_e(\chi, \zeta) := a_{\Omega_e}(H_{\hat{e} \rightarrow \Omega_e}^{\partial\Omega_e}(R_{e \rightarrow \hat{e}} \chi), H_{\hat{e} \rightarrow \Omega_e}^{\partial\Omega_e}(R_{e \rightarrow \hat{e}} \zeta)) \quad \forall \chi, \zeta \in V_e^0,$$

where \hat{e} denotes the discrete interior of the edge e and, algebraically, $R_{e \rightarrow \hat{e}}$ simply removes the degrees of freedom associated with the corners of the edge. Moreover, $H_{\hat{e} \rightarrow \Omega_e}^{\partial\Omega_e} : V_{\hat{e}} \rightarrow V_{\Omega_e}^0$ is defined as

$$a_{\Omega_e}(H_{\hat{e} \rightarrow \Omega_e}^{\partial\Omega_e} \chi, v) = 0 \quad \forall v \in V_{\Omega_e}^0, \quad H_{\hat{e} \rightarrow \Omega_e}^{\partial\Omega_e} \chi = 0 \text{ on } \partial\Omega_e, \quad H_{\hat{e} \rightarrow \Omega_e}^{\partial\Omega_e} \chi = \chi \text{ on } \hat{e};$$

hence, the upper index $\partial\Omega_e$ denotes that the harmonic extension has homogeneous Dirichlet boundary data on $\partial\Omega_e$ instead of Neumann boundary data; cf. the discussion in section 4. Finally, we denote by $\|\cdot\|_{b_e}$ and $\|\cdot\|_{d_e}$ the respective norms. We may then consider the following eigenvalue problem: find $(\psi_e^{(i)}, \mu^{(i)}) \in (V_e^0, \mathbb{R}^+)$ such that

$$(22) \quad d_e(\psi_e^{(i)}, \chi) = \mu^{(i)} b_e(\psi_e^{(i)}, \chi) \quad \forall \chi \in V_e^0.$$

We select all $n_{dir,e}$ eigenfunctions corresponding to eigenvalues below a chosen tolerance tol_{dir} and define the space

$$(23) \quad X_{dir} := \text{span}\{H_{\Gamma \rightarrow \Omega}(E_{e \rightarrow \Gamma} \psi_e^{(i)}) : e \text{ edge}, \mu^{(i)} \leq tol_{dir}\}.$$

Here, $E_{e \rightarrow \Gamma} : V_e^0 \rightarrow V_{\Gamma}^0$ extends the FE function by zero from e to Γ , and $H_{\Gamma \rightarrow \Omega} : V_{\Gamma}^0 \rightarrow V_{\Omega}^0$ is the energy-minimizing extension from the interface into the interior of the subdomains as introduced in subsection 3.2. An eigenvalue problem similar to (22) has already been considered in [28], but robustness of the resulting coarse space could not be shown theoretically.

We emphasize that none of the operators and matrices involved in (22) require any additional assembly and rely only on matrices that can be extracted from \mathbf{A} ; see section 7 for details. However, as can be seen in section 8 in Table 1, choosing $X_0 = X_{vert} \oplus X_{const} \oplus X_{dir}$ does in general not yield a robust coarse space. To obtain a (provably) robust coarse space, we introduce a second eigenvalue problem.

5.2. Transfer eigenvalue problem. To obtain a robust coarse space, we exploit a well-known a -orthogonal decomposition of $V_{\Omega_e}^3$, namely that every $u \in V_{\Omega_e}$ can be written as

$$(24) \quad u = u_{\Omega_e, \text{ha}} + u_{\Omega_e, \text{ha}}^\perp,$$

where $u_{\Omega_e, \text{ha}}^\perp \in V_{\Omega_e}^0$, and $u_{\Omega_e, \text{ha}}$ satisfies

$$(25) \quad a_{\Omega_e}(u_{\Omega_e, \text{ha}}, v) = 0 \quad \forall v \in V_{\Omega_e}^0 \quad \text{and} \quad u_{\Omega_e, \text{ha}}|_{\partial\Omega_e} = u|_{\partial\Omega_e},$$

that is, it is an energy-minimizing extension; cf. (15). The decomposition (24) is a -orthogonal, thanks to (25), and hence, we have

$$(26) \quad a_{\Omega_e}(u_{\Omega_e, \text{ha}}, u_{\Omega_e, \text{ha}}^\perp) = 0 \quad \text{and} \quad |u|_{a, \Omega_e}^2 = |u_{\Omega_e, \text{ha}}|_{a, \Omega_e}^2 + |u_{\Omega_e, \text{ha}}^\perp|_{a, \Omega_e}^2.$$

³To simplify the notation we assume here that $\partial\Omega_e \cap \partial\Omega = \emptyset$; otherwise V_{Ω_e} has to be replaced by $V_{\Omega_e}^{\partial\Omega} := \{v \in V_{\Omega_e} : v = 0 \text{ on } \partial\Omega\}$ here and henceforth.

In our approach, the eigenvalue problem from subsection 5.1 will serve to control the trace of functions in $V_{\Omega_e}^0$ on e . By introducing an eigenvalue problem on the space of functions that locally solve the PDE

$$(27) \quad V_{\Omega_e, \text{ha}} := \{w \in V_{\Omega_e} : a_{\Omega_e}(w, v) = 0 \quad \forall v \in V_{\Omega_e}^0\},$$

we can control the trace of functions in $V_{\Omega_e, \text{ha}}$ on e as well and therefore the traces of all functions in V_{Ω_e} on e . The fact that the decomposition is a -orthogonal and the right equation (26) in particular will allow us to combine the contributions from both eigenvalue problems when deriving the bound for the condition number in section 6.

The eigenvalue problem we consider on the space of local solutions of the PDE $V_{\Omega_e, \text{ha}}$ has originally been suggested in a slightly different form in the context of multiscale and localized model order reduction methods in [55]. In that paper, it has been introduced to construct interface spaces that yield a provably optimally convergent static condensation approximation of the solution of the PDE. Similar to [55] we introduce a suitable inner product $(\cdot, \cdot)_{\partial\Omega_e} : V_{\partial\Omega_e} \times V_{\partial\Omega_e} \rightarrow \mathbb{R}$, where we require that the induced norm $\|\cdot\|_{\partial\Omega_e}$ satisfies

$$(28) \quad c_1 \|\zeta\|_{\partial\Omega_e} \leq \sqrt{\alpha_{\min}} \|\zeta\|_{L^2(\partial\Omega_e)} \leq c_2 \|\zeta\|_{\partial\Omega_e} \quad \text{for all } w \in V_{\partial\Omega_e},$$

with constants c_1 and c_2 that are independent of the mesh size and the coefficient α .

Remark 5.1 (Discussion of inner product on $\partial\Omega_e$). *Based on the proof in subsection 6.3, $a_{\Omega_e}(H_{\partial\Omega_e \rightarrow \Omega_e}(\cdot), H_{\partial\Omega_e \rightarrow \Omega_e}(\cdot))$ is a natural choice as it leads to a very simple bound for the condition number. However, $a_{\Omega_e}(\cdot, \cdot)$ cannot not be computed algebraically as it requires the local Neumann matrices on Ω_e . Instead, we choose*

$$(29) \quad (\chi, \zeta)_{\partial\Omega_e} = \alpha_{\min} \frac{h}{N_{\partial\Omega_e}} (\chi, \zeta)_{l^2(\partial\Omega_e)},$$

which also satisfies (28) thanks to $\|\cdot\|_{L^2(\partial\Omega_e)}^2 \equiv \frac{h}{N_{\partial\Omega_e}} \|\cdot\|_{l^2(\partial\Omega_e)}^2$, where $N_{\partial\Omega_e}$ denotes the number of FE nodes on $\partial\Omega_e$. Note that α_{\min} , h , and $N_{\partial\Omega_e}$ are only constant scaling factors which can be included into $(\cdot, \cdot)_{\partial\Omega_e}$ or the choice of a suitable tol_{tr} . If a non-uniform triangulation is employed, h would have to be replaced by, for instance, the length of the edge $|e|$ in the equivalence of the L^2 - and l^2 -norms. We remark that even though the algebraic choice (29) yields a slightly more complicated bound of the condition number (see subsection 6.3), a numerical comparison in section 8 shows that the coarse spaces corresponding to (29) and $a_{\Omega_e}(H_{\partial\Omega_e \rightarrow \Omega_e}(\cdot), H_{\partial\Omega_e \rightarrow \Omega_e}(\cdot))$ perform very similarly; see also Fig. 5.

Next, as in [55], we introduce the transfer operator $\tilde{T} : V_{\partial\Omega_e} \rightarrow \{w|_e, w \in V_{\Omega_e, \text{ha}}\} =: V_{\Omega_e, \text{ha}, e}$ ⁴ defined as $\tilde{T}\zeta := (H_{\partial\Omega_e \rightarrow \Omega_e} \zeta)|_e$ for $\zeta \in V_{\partial\Omega_e}$, where the harmonic extension operator $H_{\partial\Omega_e \rightarrow \Omega_e} : V_{\partial\Omega_e} \rightarrow V_{\Omega_e}$ is defined as

$$a_{\Omega_e}(H_{\partial\Omega_e \rightarrow \Omega_e} \chi, v) = 0 \quad \forall v \in V_{\Omega_e}^0, \quad \text{and} \quad H_{\partial\Omega_e \rightarrow \Omega_e} \chi = \chi \quad \text{on } \partial\Omega_e;$$

cf. subsection 3.2. However, as X_{vert} , introduced in (18), already accounts for the degrees of freedom in the vertices of the coarse discretization, we wish to only take into account the behavior of the functions in the interior of e . Therefore, we define the slightly modified transfer operator $T = (I - I_{V, e})\tilde{T}$, where $I_{V, e}$ denotes the restriction of I_V to e , and consider the following transfer eigenvalue problem: Find $(\phi^{(i)}, \lambda_i) \in (V_{\Omega_e, \text{ha}}, \mathbb{R}^+)$ such that

$$(30) \quad b_e(T(\phi_e^{(i)}|_{\partial\Omega_e}), T(w|_{\partial\Omega_e})) = \lambda^{(i)} (\phi_e^{(i)}|_{\partial\Omega_e}, w|_{\partial\Omega_e})_{\partial\Omega_e} \quad \forall w \in V_{\Omega_e, \text{ha}}.$$

⁴Again for $\partial\Omega_e \cap \partial\Omega \neq \emptyset$ one needs to replace $V_{\partial\Omega_e}$ by $V_{\partial\Omega_e}^{\partial\Omega} := \{v \in V_{\partial\Omega_e} : v = 0 \text{ on } \partial\Omega\}$.

We select the eigenfunctions corresponding to the $n_{tr,e}$ largest eigenvalues such that $\lambda^{(n_{tr,e})} > tol_{tr}$ and $\lambda^{(n_{tr,e}+1)} \leq tol_{tr}$ and introduce

$$(31) \quad \varphi_e^{(i)} = T(\phi_e^{(i)}|_{\partial\Omega_e}), \quad i = 1, \dots \quad \text{and}$$

$$(32) \quad X_{tr} = \text{span}\{H_{\Gamma \rightarrow \Omega}(E_{e \rightarrow \Gamma}(\varphi_e^{(i)})) : e \text{ edge}, \lambda^{(i)} > tol_{tr}\}.$$

We highlight that thanks to (29) the calculation of the eigenfunctions of (30) only requires access to the global stiffness matrix \mathbf{A} resulting in a fully algebraic coarse space; for further details and the computational realization of (30), see section 7.

Note that we may also perform a singular value decomposition (SVD) of the operator T , which reads $T\zeta = \sum_i \sigma^{(i)} \hat{\varphi}^{(i)}(\chi^{(i)}, \zeta)|_{\partial\Omega_e}$ for $\zeta \in V_{\partial\Omega_e}$ with orthonormal bases $\hat{\varphi}^{(i)} \in V_{\Omega_e, \text{ha}, e}^0 := \{(w|_e - I_{V,e}(w|_e)), w \in V_{\Omega_e, \text{ha}}\}$, $\chi^{(i)} \in V_{\partial\Omega_e}$, and singular values $\sigma^{(i)} \in \mathbb{R}_0^+$. Then, we have, up to numerical errors, $\sigma^{(i)} = \sqrt{\lambda^{(i)}}$ and $\text{span}\{\varphi_e^{(1)}, \dots, \varphi_e^{(n)}\} = \text{span}\{\hat{\varphi}^{(1)}, \dots, \hat{\varphi}^{(n)}\}$. We can thus infer from results of the optimality of the SVD that the space $\Lambda^n = \text{span}\{\varphi_e^{(1)}, \dots, \varphi_e^{(n)}\}$ minimizes $\|T - \Pi_{\Lambda^n} T\|$ among all n -dimensional subspaces of $V_{\Omega_e, \text{ha}}^0$ and hence optimally (in the sense of Kolmogorov) approximates the range of T and thus $V_{\Omega_e, \text{ha}, e}^0$; see also [5, 50, 55].

5.3. Complete definition of the adaptive coarse space. Finally, we define the complete adaptive coarse space X_0 as

$$(33) \quad X_0 = X_{\text{VCDT}} := X_{\text{vert}} \oplus X_{\text{const}} \oplus X_{\text{dir}} \oplus X_{\text{tr}},$$

where X_{vert} , X_{const} , X_{dir} , and X_{tr} were defined in (18), (19), (23), and (32), respectively.

6. BOUND OF THE CONDITION NUMBER

As we use exact local and coarse solvers, (5) and (9), we obtain local stability with stability constant $\omega = 1$; cf. [60, Assumption 2.4] and, for the readers' convenience, Assumption SM1.1. Thanks to [60, Lemma 3.11 and follow-up discussion] and the proof of [16, Theorem 4.1], we obtain

$$(34) \quad \kappa(\mathbf{M}_{AS}^{-1} \mathbf{A}) \leq C_0^2 (m + 1),$$

where C_0^2 is the constant in the stable decomposition in Assumption 6.1 below [60, Assumption 2.2], and $m \in \mathbb{N}$ is an upper bound for the number of overlapping subdomains Ω'_i any FE node in Ω can belong to. Hence, m only depends on the structure of the overlapping domain decomposition and is, for regular domain decompositions, bounded from above; also for domain decompositions generated by mesh partitioners such as METIS [33], m is generally reasonably small. Therefore, in order to obtain a condition number bound, it is sufficient to bound the constant C_0^2 in the stable decomposition:

Assumption 6.1 (Stable decomposition [60, Assumption 2.2]). *There exists a constant C_0 , such that every $u \in V_{\Omega}^0$ admits a decomposition*

$$(35) \quad u = E_0 u_0 + \sum_{i=1}^M E_{\Omega'_i \rightarrow \Omega} u_i$$

$$(36) \quad \text{such that} \quad \sum_{i=0}^M a_{\Omega'_i}(u_i, u_i) \leq C_0^2 a_{\Omega}(u, u).$$

6.1. Construction of the stable decomposition. One key novelty of the present manuscript, which is a key ingredient for proving robustness, lies in the specific definition of the coarse component u_0 . To that end, we define projection operators

$$(37) \quad \Pi_{e,dir} v := \sum_{i=1}^{n_{dir,e}} b_e(v, \psi_e^{(i)}) \psi_e^{(i)} \quad \forall v \in V_e^0 \quad \text{and}$$

$$(38) \quad \Pi_{e,tr} v := \sum_{i=1}^{n_{tr,e}} \frac{1}{\lambda^{(i)}} b_e(v, \varphi_e^{(i)}) \varphi_e^{(i)} \quad \forall v \in V_{\Omega_e,ha,e}^0,$$

where $n_{dir,e}$ and $n_{tr,e}$ denote the number of selected eigenfunctions from the eigenproblems (22) and (30), respectively. Note that, for all $v \in V_{\Omega_e,ha,e}^0$ and $v = T(\tilde{v}|_{\partial\Omega_e})$, we have $\Pi_{e,tr} v = \sum_{i=1}^{n_{tr,e}} (\tilde{v}|_{\partial\Omega_e}, \phi^{(i)}|_{\partial\Omega_e})_{\partial\Omega_e} \varphi_e^{(i)}$, where $\phi^{(i)}$ is the i -th eigenfunction of the transfer eigenvalue problem (30). Exploiting the latter and the definition $\varphi_e^{(i)} := T(\phi_e^{(i)}|_{\partial\Omega_e})$ (see (31)) yields the expression of $\Pi_{e,tr} v$ in (38). Moreover, fitting the definition of the coarse spaces X_{dir} and X_{tr} in (23) and (32), respectively, we also introduce the maps

$$\begin{aligned} \Pi_{dir} v &:= H_{\Gamma \rightarrow \Omega}(E_{e \rightarrow \Gamma}(\Pi_{e,dir} v)) \quad \forall v \in V_e^0, \quad \text{and} \\ \Pi_{tr} v &:= H_{\Gamma \rightarrow \Omega}(E_{e \rightarrow \Gamma}(\Pi_{e,tr} v)) \quad \forall v \in V_{\Omega_e,ha,e}^0. \end{aligned}$$

Definition of the coarse interpolation. As we will later invoke Poincaré's inequality in the proof of the condition number bound, we have to include the constant function in our interpolation. In this step, we have to introduce the minimum value of the coefficient function α_{\min} into the estimate, which is why we already included it in the right-hand side of the transfer eigenvalue problem; see (28). Our final condition number bound will still be robust since the maximum eigenvalue and, hence, the contrast will not appear. Similarly as in [55], we exploit that functions which are constant on Ω_e lie in $V_{\Omega_e,ha}$. We may thus write

$$(39) \quad u|_{\Omega_e} = \widehat{u_{\Omega_e,ha}} + c_u \mathbb{1}_{\Omega_e} + u_{\Omega_e,ha}^\perp, \quad \text{where} \quad \widehat{u_{\Omega_e,ha}} := u_{\Omega_e,ha} - c_u \mathbb{1}_{\Omega_e} \in V_{\Omega_e,ha},$$

and $c_u \in \mathbb{R}$ is zero when $\partial\Omega_e \cap \partial\Omega \neq \emptyset$ and will be selected later otherwise. We define the coarse interpolation

$$(40) \quad \begin{aligned} u_0 &:= H_{\Gamma \rightarrow \Omega}((I_V u)|_\Gamma) + \sum_{e \in \Gamma} (u_{0,\Omega_e,ha} + u_{0,\Omega_e,ha}^\perp), \quad \text{where} \\ u_{0,\Omega_e,ha} &:= \Pi_{tr}(\widehat{u_{\Omega_e,ha}}|_e - I_{V,e} \widehat{u_{\Omega_e,ha}}|_e) + H_{\Gamma \rightarrow \Omega}(E_{e \rightarrow \Gamma}(c_u \mathbb{1}_e - I_{V,e} c_u \mathbb{1}_e)) \\ u_{0,\Omega_e,ha}^\perp &:= \Pi_{dir}(u_{\Omega_e,ha}^\perp|_e - I_{V,e} u_{\Omega_e,ha}^\perp|_e), \end{aligned}$$

where I_V is the interpolation by the nodal functions in X_{vert} corresponding to the vertices, and $I_{V,e}$ is the restriction of this interpolation to the edge e . To simplify notations, we assume that u_0 is already expressed in the basis of V_Ω^0 .

Definition of the local components u_i , $i = 1, \dots, M$. As typical in the proof of condition number estimates for Schwarz methods, we define

$$(41) \quad u_i = R_{\Omega \rightarrow \Omega'_i} I^h(\theta_i(u - u_0)), \quad i = 1, \dots, M,$$

where $I^h(\theta_i(u - u_0)) \in V_\Omega^0$ denotes the interpolant of $\theta_i(u - u_0)$ and $\{\theta_i\}_{i=1}^M$ is a partition of unity corresponding to an overlapping decomposition $\{\tilde{\Omega}_i\}_{i=1}^M$ of the domain Ω with overlap h ; hence, it is also a partition of unity on the overlapping domain decomposition $\{\Omega'_i\}_{i=1}^M$. In detail, we require for a FE node x_h that $\theta_i(x_h) = 1$ in Ω_i , $\theta_i(x_h) = 1/m_{x_h}$ on Γ and $\theta_i(x_h) = 0$ otherwise; here m_{x_h} denotes the number of subdomains Ω_i the FE node x_h belongs to. This definition ensures (35). See, for example, [60, Section 3.6] for the same construction with a slightly different choice of the partition of unity.

6.2. Bound of the coarse level and local contributions. The general structure of the proof follows earlier works, such as [20, 28, 29, 30]. We first prove estimates for the coarse and local components, as summarized in Lemma 6.2, and then combine them to the final estimate for C_0^2 in Proposition 6.6 in subsection 6.4. Plugged into (34), we obtain the final condition number estimate. The main step in the proof is finding an upper bound for the term $|E_{e \rightarrow \Omega_e} [(u - u_0)|_e]|_{a, \Omega_e}^2$. This corresponds to upper bounds for $|w_{e_{ij}}(u - u_0)|_{a, \Omega_e}^2$ in OS-ACMS [28] or $|z_{\xi \rightarrow \Omega_\xi}(u - u_0)|_{a, \Omega_\xi}^2$ in AGDSW [27], respectively; for details, see the corresponding references. The proof of this bound differs significantly for our new method and is the central novel contribution of this manuscript in terms of numerical analysis and the topic of the next subsection. The remainder of the proof of the bound of the coarse level and local contributions, as summarized in Lemma 6.2, is standard. It follows the earlier works listed above, and can, for the readers' convenience, be found in subsection SM1.1.

Lemma 6.2 (Bound of the coarse level and local contributions). *Let u_0 and u_i be defined as in (40) and (41), respectively, and let m_e denote the maximal number of edges e in a subdomain Ω_i . Then, we have*

$$(42) \quad |u_0|_{a, \Omega}^2 \leq 2|u|_{a, \Omega}^2 + 2m_e \sum_{i=1}^M \sum_{e \subset \partial \Omega_i} |E_{e \rightarrow \Omega_e} [(u - u_0)|_e]|_{a, \Omega_e}^2,$$

$$(43) \quad \sum_{i=1}^M |u_i|_{a, \Omega'_i}^2 \leq 18|u|_{a, \Omega}^2 + 15m_e \sum_{i=1}^M \sum_{e \subset \partial \Omega_i} |E_{e \rightarrow \Omega_e} [(u - u_0)|_e]|_{a, \Omega_e}^2,$$

where $E_{e \rightarrow \Omega_e}$ has been defined in the beginning of subsection 5.1.

6.3. Bound of the extension of $(u - u_0)|_e$. To complete the proof of the bound of the condition number it thus remains to estimate the term $|E_{e \rightarrow \Omega_e} [(u - u_0)|_e]|_{a, \Omega_e}^2$, which is the topic of this subsection. Different from other approaches, we decompose V_{Ω_e} in an a -orthogonal way and derive a bound for each part separately. Since the decomposition is a -orthogonal, we are finally able to combine both parts again. In particular, as already indicated in subsection 5.2 and more specifically in (24), we exploit that every $u \in V_{\Omega_e}$ can be written as

$$(44) \quad u = u_{\Omega_e, \text{ha}} + u_{\Omega_e, \text{ha}}^\perp,$$

where $u_{\Omega_e, \text{ha}}^\perp \in V_{\Omega_e}^0$ and $u_{\Omega_e, \text{ha}}$ satisfies

$$(45) \quad a_{\Omega_e}(u_{\Omega_e, \text{ha}}, v) = 0 \quad \forall v \in V_{\Omega_e}^0, \quad \text{and} \quad u_{\Omega_e, \text{ha}}|_{\partial \Omega_e} = u|_{\partial \Omega_e}.$$

Thanks to the definition of the coarse level contribution in (40), $u_{0, \Omega_e, \text{ha}}|_{e^*} = 0$ and $u_{0, \Omega_e, \text{ha}}^\perp|_{e^*} = 0$ for $e \neq e^*$, and the linearity of the interpolation operator I_V , we may then split the term $|E_{e \rightarrow \Omega_e} [(u - u_0)|_e]|_{a, \Omega_e}^2$ as follows

$$(46) \quad |E_{e \rightarrow \Omega_e} [(u - u_0)|_e]|_{a, \Omega_e}^2 \leq 2 \left| E_{e \rightarrow \Omega_e} [(u_{\Omega_e, \text{ha}} - I_V u_{\Omega_e, \text{ha}} - u_{0, \Omega_e, \text{ha}})|_e] \right|_{a, \Omega_e}^2$$

$$(47) \quad + 2 \left| E_{e \rightarrow \Omega_e} [(u_{\Omega_e, \text{ha}}^\perp - I_V u_{\Omega_e, \text{ha}}^\perp - u_{0, \Omega_e, \text{ha}}^\perp)|_e] \right|_{a, \Omega_e}^2.$$

Next, by exploiting the properties of the eigenvalue problems introduced in subsections 5.1 and 5.2, we will estimate the terms in (46) and (47) separately, and combine the estimate at the end by exploiting a -orthogonality, that is,

$$(48) \quad |u|_{a, \Omega_e}^2 = |u_{\Omega_e, \text{ha}}|_{a, \Omega_e}^2 + |u_{\Omega_e, \text{ha}}^\perp|_{a, \Omega_e}^2.$$

Bound of the harmonic part. To estimate the terms containing the harmonic part of u , we will make use of the fact that the space $\Lambda_n = \text{span}\{\varphi_e^{(1)}, \dots, \varphi_e^{(n)}\}$ minimizes $\|T - \Pi_{e,tr}T\|$ among all n -dimensional subspaces of $V_{\Omega_e, \text{ha}}^0$ (see last paragraph of subsection 5.2 for the definition) and that for all $v \in V_{\Omega_e, \text{ha}, e} = \{w|_e, w \in V_{\Omega_e, \text{ha}}\}$ we have

$$(49) \quad \|(v|_e - I_{V,e}(v|_e)) - \Pi_{e,tr}(v|_e - I_{V,e}(v|_e))\|_{b_e} \leq \sqrt{\text{tol}_{tr}} \|v|_{\partial\Omega_e}\|_{\partial\Omega_e}.$$

This result follows from the well-known fact that $\|T - \Pi_{e,tr}T\| = \sigma_{n_{tr,e}+1}$ as Λ_n is the span of the first n left singular vectors of T ; cf. the Eckart-Young theorem, for instance, in [22] for the discrete setting and Theorem 2.2 in Chapter 4 in [50] for infinite-dimensional spaces, and [5, 55] for how to use this result to derive error bounds for the local and global approximation error of optimally converging multiscale methods. We may then show the following result.

Proposition 6.3 (Bound of the harmonic part). *Let the constants $c_{t,e}$ and $c_{p,e}$ be defined as*

$$(50) \quad c_{t,e} := \sup_{v \in V_{\Omega_e, \text{ha}}} \frac{\|v|_{\partial\Omega_e}\|_{L^2(\partial\Omega_e)}}{\|v\|_{H^1(\Omega_e)}}, \quad c_{p,e} := \sup_{v \in V_{\Omega_e, \text{ha}}} \frac{\|v - \frac{c_{\Omega_e}}{|\Omega_e|} \int_{\Omega_e} v \mathbb{1}_{\Omega_e}\|_{L^2(\Omega_e)}}{\|\nabla v\|_{L^2(\Omega_e)}},$$

where $c_{\Omega_e} = 1$ if $\partial\Omega_e \cap \partial\Omega = \emptyset$ and 0 otherwise. Then, we have

$$(51) \quad \left| E_{e \rightarrow \Omega_e} [(u_{\Omega_e, \text{ha}} - I_V u_{\Omega_e, \text{ha}} - u_{0, \Omega_e, \text{ha}})|_e] \right|_{a, \Omega_e}^2 \leq \frac{c_{t,e}^2 \text{tol}_{tr} (1 + c_{p,e}^2)}{c_1^2} |u_{\Omega_e, \text{ha}}|_{a, \Omega_e}^2,$$

where c_1 depends on the choice of the bilinear form $(\cdot, \cdot)_{\partial\Omega_e}$ in (29); see (28).

Proof. By exploiting the definition of $u_{0, \Omega_e, \text{ha}}$ in (40), the restriction to the edge e , the linearity of the interpolation operators I_V and $I_{V,e}$, the definition of $\widehat{u_{\Omega_e, \text{ha}}}$ in (39), and the definition of the inner product b_e in (20), we obtain

$$\begin{aligned} & \left| E_{e \rightarrow \Omega_e} \left[\left(u_{\Omega_e, \text{ha}} - I_V u_{\Omega_e, \text{ha}} - u_{0, \Omega_e, \text{ha}} \right) \Big|_e \right] \right|_{a, \Omega_e}^2 \\ &= \left| E_{e \rightarrow \Omega_e} \left[\left(u_{\Omega_e, \text{ha}} - I_V u_{\Omega_e, \text{ha}} - \Pi_{tr}(\widehat{u_{\Omega_e, \text{ha}}}|_e - I_{V,e}\widehat{u_{\Omega_e, \text{ha}}}|_e) \right. \right. \right. \\ & \quad \left. \left. - H_{\Gamma \rightarrow \Omega}(E_{e \rightarrow \Gamma}(c_u \mathbb{1}_e - I_{V,e}c_u \mathbb{1}_e)) \right) \Big|_e \right] \right|_{a, \Omega_e}^2 \\ &= \left| E_{e \rightarrow \Omega_e} \left[\left(u_{\Omega_e, \text{ha}}|_e - I_{V,e}u_{\Omega_e, \text{ha}}|_e - \Pi_{e,tr}(\widehat{u_{\Omega_e, \text{ha}}}|_e - I_{V,e}\widehat{u_{\Omega_e, \text{ha}}}|_e) \right. \right. \right. \\ & \quad \left. \left. - (c_u \mathbb{1}_e - I_{V,e}c_u \mathbb{1}_e) \right) \Big|_e \right] \right|_{a, \Omega_e}^2 \\ &= \left| E_{e \rightarrow \Omega_e} \left[\left(\widehat{u_{\Omega_e, \text{ha}}}|_e - I_{V,e}\widehat{u_{\Omega_e, \text{ha}}}|_e - \Pi_{e,tr}(\widehat{u_{\Omega_e, \text{ha}}}|_e - I_{V,e}\widehat{u_{\Omega_e, \text{ha}}}|_e) \right) \right] \right|_{a, \Omega_e}^2 \\ &= \left\| \left(\widehat{u_{\Omega_e, \text{ha}}}|_e - I_{V,e}\widehat{u_{\Omega_e, \text{ha}}}|_e - \Pi_{e,tr}(\widehat{u_{\Omega_e, \text{ha}}}|_e - I_{V,e}\widehat{u_{\Omega_e, \text{ha}}}|_e) \right) \right\|_{b_e}^2. \end{aligned}$$

As $\widehat{u_{\Omega_e, \text{ha}}}|_e$ is in $V_{\Omega_e, \text{ha}, e} = \{w|_e, w \in V_{\Omega_e, \text{ha}}\}$, we may then invoke (49) and obtain

$$(52) \quad \left| E_{e \rightarrow \Omega_e} \left[\left(u_{\Omega_e, \text{ha}} - I_V u_{\Omega_e, \text{ha}} - u_{0, \Omega_e, \text{ha}} \right) \Big|_e \right] \right|_{a, \Omega_e}^2 \leq \text{tol}_{tr} \|\widehat{u_{\Omega_e, \text{ha}}}|_{\partial\Omega_e}\|_{\partial\Omega_e}^2.$$

To conclude the estimate of the harmonic part of the function, we exploit (28) and choose c_u in $\widehat{u_{\Omega_e, \text{ha}}} := u_{\Omega_e, \text{ha}} - c_u \mathbb{1}_{\Omega_e}$ as $c_u = (1/|\Omega_e|) \int_{\Omega_e} u_{\Omega_e, \text{ha}}$ if $\partial\Omega_e \cap \partial\Omega = \emptyset$ and $c_u = 0$

otherwise. Now, we apply the trace theorem and the Poincaré inequality:

$$\begin{aligned}
& \left| E_{e \rightarrow \Omega_e} \left[\left(u_{\Omega_e, \text{ha}} - I_V u_{\Omega_e, \text{ha}} - u_{0, \Omega_e, \text{ha}} \right) \Big|_e \right] \right|_{a, \Omega_e}^2 \\
& \leq \text{tol}_{tr} \|\widehat{u_{\Omega_e, \text{ha}}}\|_{\partial \Omega_e}^2 \leq \text{tol}_{tr} \frac{\alpha_{min}}{c_1^2} \|\widehat{u_{\Omega_e, \text{ha}}}\|_{L^2(\partial \Omega_e)}^2 \\
& \leq \text{tol}_{tr} \frac{c_{t,e}^2 \alpha_{min}}{c_1^2} (\|\widehat{u_{\Omega_e, \text{ha}}}\|_{L^2(\Omega_e)}^2 + \|\nabla \widehat{u_{\Omega_e, \text{ha}}}\|_{L^2(\Omega_e)}^2) \\
& \leq \text{tol}_{tr} \frac{c_{t,e}^2 \alpha_{min}}{c_1^2} (c_{p,e}^2 \|\nabla u_{\Omega_e, \text{ha}}\|_{L^2(\Omega_e)}^2 + \|\nabla \widehat{u_{\Omega_e, \text{ha}}}\|_{L^2(\Omega_e)}^2) \\
& = \text{tol}_{tr} \frac{c_{t,e}^2 \alpha_{min}}{c_1^2} (1 + c_{p,e}^2) \|\nabla u_{\Omega_e, \text{ha}}\|_{L^2(\Omega_e)}^2 \leq \frac{c_{t,e}^2 \text{tol}_{tr}}{c_1^2} (1 + c_{p,e}^2) |u_{\Omega_e, \text{ha}}|_{a, \Omega_e}^2.
\end{aligned}$$

□

Bound of the perpendicular part. By exploiting that the eigenfunctions $\psi_e^{(i)}$, $i = 1, \dots, \dim(V_e^0)$, of (22) span V_e^0 and that we select all $n_{dir,e}$ eigenfunctions corresponding to eigenvalues below a chosen tolerance tol_{dir} to define the space X_{dir} , we obtain by standard spectral arguments for adaptive coarse spaces that

$$(53) \quad \|v\|_{d_e}^2 = \|\Pi_{e,dir} v\|_{d_e}^2 + \|v - \Pi_{e,dir} v\|_{d_e}^2, \quad \|v - \Pi_{e,dir} v\|_{b_e}^2 \leq \frac{1}{\text{tol}_{dir}} \|v - \Pi_{e,dir} v\|_{d_e}^2,$$

for each $v \in V_e^0$; cf. , e.g., [37, 38, 58, 28, 29]. Using these two results, we may prove the following result.

Proposition 6.4 (Bound of the perpendicular part). *We have*

$$(54) \quad \left| E_{e \rightarrow \Omega_e} \left[\left(u_{\Omega_e, \text{ha}}^\perp - I_V u_{\Omega_e, \text{ha}}^\perp - u_{0, \Omega_e, \text{ha}}^\perp \right) \Big|_e \right] \right|_{a, \Omega_e}^2 \leq \frac{1}{\text{tol}_{dir}} |u_{\Omega_e, \text{ha}}^\perp|_{a, \Omega_e}^2.$$

Proof. By exploiting the definition of $u_{0, \Omega_e, \text{ha}}^\perp$ in (40), the restriction to the edge e , the linearity of the interpolation operators I_V and $I_{V,e}$, the definition of the inner product b_e in (20), and (53), we obtain

$$\begin{aligned}
& \left| E_{e \rightarrow \Omega_e} \left[\left(u_{\Omega_e, \text{ha}}^\perp - I_V u_{\Omega_e, \text{ha}}^\perp - u_{0, \Omega_e, \text{ha}}^\perp \right) \Big|_e \right] \right|_{a, \Omega_e}^2 \\
& = \left| E_{e \rightarrow \Omega_e} \left[\left(u_{\Omega_e, \text{ha}}^\perp - I_V u_{\Omega_e, \text{ha}}^\perp - \Pi_{dir}(u_{\Omega_e, \text{ha}}^\perp|_e - I_{V,e} u_{\Omega_e, \text{ha}}^\perp|_e) \right) \Big|_e \right] \right|_{a, \Omega_e}^2 \\
& = \left| E_{e \rightarrow \Omega_e} \left[\left((u_{\Omega_e, \text{ha}}^\perp|_e - I_{V,e} u_{\Omega_e, \text{ha}}^\perp|_e) - \Pi_{e,dir}(u_{\Omega_e, \text{ha}}^\perp|_e - I_{V,e} u_{\Omega_e, \text{ha}}^\perp|_e) \right) \Big|_e \right] \right|_{a, \Omega_e}^2 \\
& = \|(u_{\Omega_e, \text{ha}}^\perp|_e - I_{V,e} u_{\Omega_e, \text{ha}}^\perp|_e) - \Pi_{e,dir}(u_{\Omega_e, \text{ha}}^\perp|_e - I_{V,e} u_{\Omega_e, \text{ha}}^\perp|_e)\|_{b_e}^2 \\
& \stackrel{(53)}{\leq} \frac{1}{\text{tol}_{dir}} \|u_{\Omega_e, \text{ha}}^\perp|_e - I_{V,e} u_{\Omega_e, \text{ha}}^\perp|_e\|_{d_e}^2.
\end{aligned}$$

A close inspection of the definition of the inner product d_e in (21) reveals that, as we have $R_{e \rightarrow \dot{e}}(u_{\Omega_e, \text{ha}}^\perp|_e - I_{V,e} u_{\Omega_e, \text{ha}}^\perp|_e) = R_{e \rightarrow \dot{e}}(u_{\Omega_e, \text{ha}}^\perp|_e)$, there holds

$$\|u_{\Omega_e, \text{ha}}^\perp|_e - I_{V,e} u_{\Omega_e, \text{ha}}^\perp|_e\|_{d_e}^2 = a_{\Omega_e} (H_{\dot{e} \rightarrow \Omega_e}^{\partial \Omega_e} R_{e \rightarrow \dot{e}}(u_{\Omega_e, \text{ha}}^\perp|_e), H_{\dot{e} \rightarrow \Omega_e}^{\partial \Omega_e} R_{e \rightarrow \dot{e}}(u_{\Omega_e, \text{ha}}^\perp|_e)).$$

As $u_{\Omega_e, \text{ha}}^\perp \in V_{\Omega_e}^0$ and the discrete harmonic extension $H_{\dot{e} \rightarrow \Omega_e}^{\partial \Omega_e} R_{e \rightarrow \dot{e}}(u_{\Omega_e, \text{ha}}^\perp|_e)$ minimizes the $|\cdot|_{a, \Omega_e}$ -norm among all functions in $V_{\Omega_e}^0$ that equal $u_{\Omega_e, \text{ha}}^\perp$ on \dot{e} , we conclude that

$$\|u_{\Omega_e, \text{ha}}^\perp|_e - I_{V,e} u_{\Omega_e, \text{ha}}^\perp|_e\|_{d_e}^2 \leq |u_{\Omega_e, \text{ha}}^\perp|_{a, \Omega_e}^2.$$

□

Combining the bounds of the harmonic and perpendicular parts. By invoking the stability result (48) and exploiting the estimate (46)-(47), Proposition 6.3, and Proposition 6.4, we obtain the following result.

Corollary 6.5. *We have*

$$|E_{e \rightarrow \Omega_e} [(u - u_0)|_e]|_{a, \Omega_e}^2 \leq 2 \max \left\{ \frac{c_{t,e}^2 \text{tol}_{tr}(1 + c_{p,e}^2)}{c_1^2}, \frac{1}{\text{tol}_{dir}} \right\} |u|_{a, \Omega_e}^2.$$

6.4. Complete bound of the condition number. By combining Lemma 6.2 and Corollary 6.5, we obtain the following bound for the condition number:

Proposition 6.6. *Let u_0 and u_i , $i = 1, \dots, M$ be defined as in (40) and (41), respectively. Let further m_e denote the maximal number of edges e in a subdomain Ω_i , $\nu := \max_{e \in \Gamma} \{\text{number of subdomains } \Omega_i \text{ that satisfy } \Omega_i \cap \hat{e} \neq \emptyset\}$, $\tilde{\omega} = \max_{i=1, \dots, M} \{\text{number of } \Omega_e \text{ such that } \Omega_e \cap \Omega_i \neq \emptyset\}$, $c_t := \max_{e \in \Gamma} c_{t,e}$, and $c_p := \max_{e \in \Gamma} c_{p,e}$, where $c_{t,e}$ and $c_{p,e}$ have been defined in (50). Then, the condition number can be bounded as $\kappa(\mathbf{M}_{AS}^{-1} \mathbf{A}) \leq C_0^2 (m + 1)$ with*

$$(55) \quad C_0^2 := \left(20 + 34m_e \nu \tilde{\omega} \max \left\{ \frac{c_t^2 \text{tol}_{tr}(1 + c_p^2)}{c_1^2}, \frac{1}{\text{tol}_{dir}} \right\} \right)$$

in the stable decomposition in Assumption 6.1.

7. COMPUTATIONAL REALIZATION

In this section, we briefly discuss the algorithmic steps for the algebraic construction of the different components of the two level Schwarz preconditioner (10) with the adaptive coarse space X_0 (33). As $X_{\text{GDSW}} = X_{\text{vert}} \oplus X_{\text{const}} \subset X_0$ (see discussion at the beginning of section 5), many algorithmic building blocks are the same as in the standard GDSW preconditioner. We thus mainly focus here on the Dirichlet and transfer eigenvalue problems and refer to [32, 26] for details on the algebraic construction of GDSW preconditioners.

The main algorithmic components of the two-level preconditioner (10). Since $\mathbf{E}_{\Omega'_i \rightarrow \Omega} = \mathbf{R}_{\Omega \rightarrow \Omega'_i}^T$, $\mathbf{E}_0 = \mathbf{R}_0^T$ and thus $\mathbf{A}_{\Omega'_i} = \mathbf{R}_{\Omega \rightarrow \Omega'_i} \mathbf{A} \mathbf{R}_{\Omega \rightarrow \Omega'_i}^T$, and $\mathbf{A}_0 = \mathbf{R}_0 \mathbf{A} \mathbf{R}_0^T$, it is sufficient to construct the operators $\mathbf{R}_{\Omega \rightarrow \Omega'_i}$, for $i = 1, \dots, M$, and \mathbf{R}_0 .

Nonoverlapping domain decomposition. Let us assume that a nonoverlapping domain decomposition $\bar{\Omega} = \cup_i \bar{\Omega}_i$ is already given or can be obtained from the sparsity pattern of the matrix \mathbf{A} using a graph partitioner, such as METIS [34].

Restriction operators on the first level. For the first level, the operators $\mathbf{R}_{\Omega \rightarrow \Omega'_i}$ extract the subvector corresponding to Ω'_i when applied to a global FE vector. Similarly, $\mathbf{A}_{\Omega'_i} = \mathbf{R}_{\Omega \rightarrow \Omega'_i} \mathbf{A} \mathbf{R}_{\Omega \rightarrow \Omega'_i}^T$ can be obtained by extracting the submatrix corresponding to Ω'_i from \mathbf{A} . Hence, the $\mathbf{R}_{\Omega \rightarrow \Omega'_i}$ never have to be set up explicitly.

To determine the action of the operators $\mathbf{R}_{\Omega \rightarrow \Omega'_i}$, it is sufficient to identify the index sets of the subdomains Ω'_i . Starting from the nonoverlapping subdomains Ω_i , the overlapping subdomains can be constructed recursively by adding layers of FE nodes. This can, again, be performed based on the sparsity pattern of \mathbf{A} , making use of the fact that two FE nodes with indices k and l share a nonzero off-diagonal coefficient in \mathbf{A} if they are adjacent.

Computation of the coarse basis functions. The coarse basis functions in terms of the FE basis functions are stored in the columns of \mathbf{E}_0 . If we have computed the interface values $\mathbf{E}_{0,\Gamma}$ of the coarse basis functions, the interior values are then computed as energy-minimizing extensions from the interface to the interior of the subdomains $\mathbf{E}_{0,I} = -\mathbf{A}_{II}^{-1} \mathbf{A}_{I\Gamma} \mathbf{E}_{0,\Gamma}$; cf. (15) and (16) and the discussion in subsection 3.2.

The steps above depend on a partition of the nodes into interior and interface nodes. This can be performed based on the multiplicity of the nodes in the nonoverlapping domain

decomposition: FE nodes which belong to only one subdomain are the interior nodes, whereas nodes which belong to two subdomains are the edge nodes, and nodes which belong to more than two subdomains are the vertices. Then, the interface nodes are the union of the edge and vertex nodes. Hence, the nodes can be categorized algebraically, just based on the nonoverlapping domain decomposition.

7.1. Algebraic construction of coarse edge functions from Dirichlet and transfer eigenvalue problem.

Construction of Ω_e . Both eigenvalue problems require the oversampling domain Ω_e corresponding to each edge e . It can be constructed in a similar way as the overlapping subdomains: we start with the FE nodes of interior of the edge e and extend the set recursively layer-by-layer of elements; cf. Fig. 3. As before, this can be done based on the sparsity pattern of \mathbf{A} .

Dirichlet eigenvalue problem (22). The Dirichlet eigenvalue problems can be written as: Find $(\mathbf{v}, \mu) \in \mathbb{R}^{N_{\hat{e}}} \times \mathbb{R}^+$, such that

$$\mathbf{S}_e \mathbf{v} = \mu \mathbf{A}_{\hat{e}\hat{e}} \mathbf{v}$$

with matrices \mathbf{S}_e and $\mathbf{A}_{\hat{e}\hat{e}}$; see also (17). The latter can easily be extracted from \mathbf{A} ; it is the submatrix corresponding to the interior edge nodes. The Schur complement on the left-hand side is given by $\mathbf{S}_e = \mathbf{A}_{\hat{e}\hat{e}} - \mathbf{A}_{\hat{e}\tilde{R}} \mathbf{A}_{\tilde{R}\tilde{R}}^{-1} \mathbf{A}_{\tilde{R}\hat{e}}$, where the index set \tilde{R} corresponds to the interior nodes of Ω_e except for the interior nodes of e . As $\mathbf{A}_{\hat{e}\hat{e}}$, the matrices $\mathbf{A}_{\hat{e}\tilde{R}}$, $\mathbf{A}_{\tilde{R}\tilde{R}}$, and $\mathbf{A}_{\tilde{R}\hat{e}}$ can be extracted as submatrices of \mathbf{A} .

Transfer eigenvalue problem (30). The transfer eigenvalue problem can be written in matrix form as: Find $(\mathbf{v}, \lambda) \in \mathbb{R}^{N_{\partial\Omega_e}} \times \mathbb{R}^+$, such that

$$\mathbf{T}^T \mathbf{A}_{\hat{e}\hat{e}} \mathbf{T} \mathbf{v} = \lambda \frac{\alpha_{\min}}{N_{\partial\Omega_e}} \mathbf{I}_{\partial\Omega_e} \mathbf{v}$$

where \mathbf{T} is the matrix corresponding to the transfer operator, $N_{\partial\Omega_e}$ is the number of FE nodes on $\partial\Omega_e$, and $\mathbf{I}_{\partial\Omega_e} \in \mathbb{R}^{N_{\partial\Omega_e} \times N_{\partial\Omega_e}}$ is the identity matrix on the degrees of freedom of $\partial\Omega_e$. Therefore, let

$$\hat{\mathbf{T}} = \begin{pmatrix} -\mathbf{A}_{\hat{\Omega}_e \hat{\Omega}_e}^{-1} \mathbf{A}_{\hat{\Omega}_e \partial\Omega_e} \\ \mathbf{I}_{\partial\Omega_e} \end{pmatrix},$$

where $\hat{\Omega}_e$ and $\partial\Omega_e$ correspond to the interior nodes of Ω_e and the nodes on $\partial\Omega_e$, respectively. This corresponds to the energy-minimizing extension from $\partial\Omega_e$ to Ω_e ; cf. (16). Then, $\mathbf{T} = \mathbf{R}_{\Omega_e \rightarrow \hat{e}} \hat{\mathbf{T}}$, where \hat{e} denotes the discrete interior of e . Again, all matrices involved in the transfer eigenvalue problem, $\mathbf{A}_{\hat{e}\hat{e}}$, $\mathbf{A}_{\hat{\Omega}_e \hat{\Omega}_e}$, and $\mathbf{A}_{\hat{\Omega}_e \partial\Omega_e}$, can be extracted from \mathbf{A} , and $\mathbf{R}_{\Omega_e \rightarrow \hat{e}}$ only requires the index sets of Ω_e and \hat{e} .

Remark 7.1. *We can efficiently approximate the space spanned by the leading singular vectors of the transfer operator T by using randomization as suggested in [9] in the context of localized model reduction. This is helpful since the transfer eigenvalue problem, which is defined on the nodes of $\partial\Omega_e$, may be significantly larger than the Dirichlet eigenvalue problem, which is defined on the interior nodes of e .*

Orthogonalization of the edge functions. Let us remark that $V_{\Omega_e}^0|_e \cap V_{\Omega_e, \text{ha}}|_e \neq \emptyset$. Hence, even though the two spaces are a -orthogonal on Ω_e , when restricted to an edge, the functions from the two spaces may not be linearly independent anymore. In order to remove (almost) linearly dependent edge functions, we finally orthogonalize the edge functions for each edge using a proper orthogonal decomposition (POD) [8, 54].

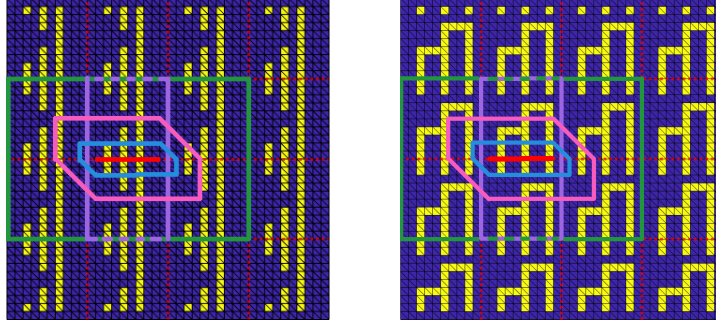


FIGURE 3. Heterogeneous coefficient functions with high-coefficient channels of varying lengths (**left**) and comb-type high-coefficient components (**right**) cutting the edges on a 4×4 subdomains with $H/h = 10$ and different choices of oversampling domains Ω_e : the domain decomposition interface is depicted as dashed red lines, the elements with $\alpha = \alpha_{\max}$ are colored yellow, and the elements with $\alpha = \alpha_{\min}$ are colored dark blue. In addition, the oversampling domain Ω_e^{2h} is depicted in light blue, Ω_e^{5h} in pink, Ω_e^H in light green, and the domain for the extensions in AGDSW eigenvalue problems in light purple; the discrete interior edge \tilde{e} is plotted in solid red.

8. NUMERICAL RESULTS

In this section, we present numerical results demonstrating the robustness of our new adaptive coarse space in (33). In particular, we consider the heterogeneous model problem (1) with coefficient function α introduced in section 2 on the computational domain $\Omega = [0, 1]^2$. We use piecewise linear finite elements on a regular mesh to discretize and obtain (3). Moreover, we use the preconditioned conjugate gradient (PCG) method and stop the iteration once $\|\mathbf{M}^{-1}r^{(k)}\|/\|\mathbf{M}^{-1}r^{(0)}\| < 10^{-10}$. The overlapping domain decomposition into $\{\Omega'_i\}_{i=1}^M$ is done in a structured way, resulting in square subdomains. In all numerical experiments, we will use an algebraic overlap of $1h$, that is, we extend the nonoverlapping subdomains by one layer of finite element nodes to obtain the overlapping subdomains. Moreover, we keep the threshold for the selection of eigenfunctions in the Dirichlet eigenvalue problem $tol_{dir} = 10^{-3}$ and the tolerance for the POD orthogonalization $tol_o = 10^{-5}$ fixed. The threshold for the transfer eigenvalue problem tol_{tr} is chosen as 10^5 in most cases and only varied in a few cases as reported in the tables. The algorithms have been implemented and run using MATLAB_R2021a.

We compare the adaptive coarse space proposed in this paper in (33) and variants of it with the classical two-level GDSW coarse space and AGDSW coarse spaces. Even though our theory holds for general coefficient functions, we are mostly interested in testing our coarse space for difficult configurations, where standard coarse spaces fail. Let us briefly comment on the design of the coefficient functions. We concentrate on discontinuous coefficient functions instead of continuously varying coefficient functions since large coefficient jumps at the domain decomposition interface have a stronger influence on the convergence; this is also reflected by the results in subsection 8.5. Furthermore, it is well-known that coefficient jumps inside the subdomains have only a minor influence; see, for example [21]. It has also been observed that those examples where the high coefficient components do not touch the Dirichlet boundary of the domain are the more difficult ones; this behavior is particularly evident for low numbers of subdomains. Therefore, except for the realistic coefficient function in subsection 8.5, we set one layer of elements with low coefficient at the boundary of the domain.

X_0	Ω_{out}	tol_{tr}	$\dim X_0$	κ	# its.
X_{GDSW}	–	–	33 / 33	$2.7 \cdot 10^5$	118
X_{AGDSW}	–	–	57 / 57	7.4	24
X_{VCD}	Ω_e^{2h}	–	33 / 33	$2.7 \cdot 10^5$	118
	Ω_e^{5h}	–	57 / 57	7.2	24
	Ω_e^H	–	57 / 57	7.2	24
$X_{\text{VCT-}l^2}$	Ω_e^{2h}	10^5	93 / 105	7.6	24
	Ω_e^{5h}	10^5	57 / 66	19.0	36
	Ω_e^H	10^5	57 / 66	19.0	36
$X_{\text{VCDT-}l^2}$	Ω_e^{2h}	10^5	93 / 105	7.6	24
	Ω_e^{5h}	10^6	57 / 69	7.6	24
	Ω_e^{5h}	10^5	57 / 90	7.2	25
	Ω_e^H	10^5	57 / 90	7.2	24
$X_{\text{VCDT-}a}$	Ω_e^{2h}	10^5	57 / 69	7.5	24
	Ω_e^{5h}	10^5	57 / 72	7.2	24
	Ω_e^H	10^5	57 / 69	7.3	24

TABLE 1. Numerical results for the coefficient function shown in Fig. 3 (left), 4×4 subdomains with $H/h = 10$, and $\alpha_{\max} = 10^6$ and $\alpha_{\min} = 1$ using different coarse spaces; in case of the novel coarse spaces $X_{\text{VCDT-}*}$, we vary the size of Ω_e : two layers of finite elements (Ω_e^{2h}), five layers of finite elements (Ω_e^{5h}), or one layer of subdomains (Ω_e^H) around e ; see also Fig. 3 (left); for the Ω_e^{2h} case, we vary the threshold tol_{tr} . We report the coarse space dimension (final dimension / dimension before POD orthogonalization), the estimated condition number, and the iteration count. Non-default tolerances tol_{tr} are marked in **bold face**.

8.1. A first model problem: Channels of varying lengths. As a first model problem, we consider the coefficient function shown in Fig. 3 (left). The results are listed in Table 1, where here and elsewhere the reported condition number is an estimate from the Lanczos process within PCG. They clearly indicate that the condition number for the classical coarse space is not robust with respect to the contrast of the coefficient function; in fact, the condition number of $2.7 \cdot 10^5$ is close to the contrast $\alpha_{\max}/\alpha_{\min} = 10^6$ itself. Due to the moderate number of subdomains, the resulting iteration count is still moderate, that is, 118.

Both the AGDW and the new coarse space are robust, resulting in a condition number below 10 and an iteration count of 24 or 25. This is the case for both the fully algebraic variant ($X_{\text{VCDT-}l^2}$) and the variant that uses the a bilinear form ($X_{\text{VCDT-}a}$). The latter two yield comparable results, also when varying the size of Ω_e from two layers of elements (Ω_e^{2h}), to five layers of elements (Ω_e^{5h}) and one layer of subdomains (Ω_e^H) around the edge e ; cf. Fig. 3 (left) for plots of the different choices of Ω_e .

In Table 1, we also provide results for only using one of the two eigenvalue problems, that is either only the Dirichlet eigenvalue problem (X_{VCD}) or only the transfer eigenvalue problem ($X_{\text{VCT-}l^2}$). We observe that, once Ω_e gets too small (Ω_e^{2h}), the Dirichlet eigenvalue problem fails to detect the high-coefficient channels. The resulting coarse space just corresponds to the standard GDSW coarse space. On the other hand, for this example, the transfer eigenvalue problem alone already yields a robust coarse space.

Figure 4 shows the eigenvalue distribution for the Dirichlet and transfer eigenvalue problems of $X_{\text{VCDT-}l^2}$ for varying the size of Ω_e . We observe that, for a smaller Ω_e , the eigenvalues are much more concentrated in certain parts of the spectrum. For a larger choice of Ω_e , they are more distributed across the spectrum. The eigenmodes necessary for obtaining robustness can be identified by the gap in the spectrum, which should contain the threshold.

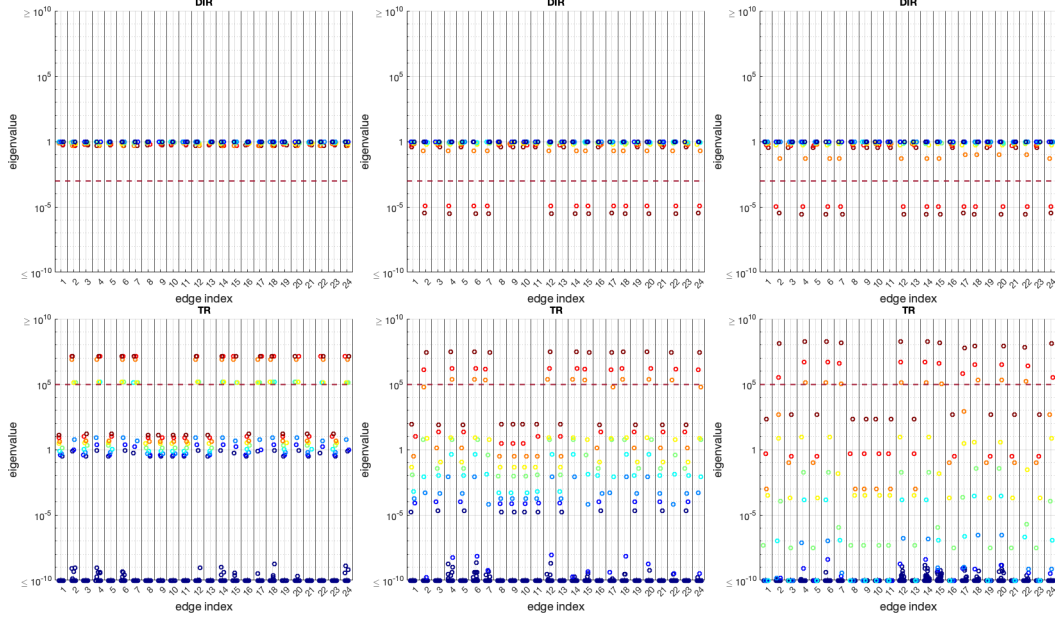


FIGURE 4. Eigenvalue distributions for the Dirichlet (top) and transfer (bottom) eigenvalue problems for configuration in Fig. 3 (left) for different sizes of Ω_e : Ω_e^{2h} (left), Ω_e^{5h} (middle), and Ω_e^H (right); see also Fig. 3 (left). Threshold of 10^{-3} and 10^{-5} for the Dirichlet and transfer eigenvalue problems are plotted as dashed red lines. Note that all eigenvalues below 10^{-10} or larger than 10^{10} are plotted as 10^{-10} or 10^{10} , respectively. The eigenvalues are colored based on their ordering, from the largest eigenvalue (red) to the smallest eigenvalue (blue).

Choosing a larger threshold for the Dirichlet eigenvalue problem and smaller threshold for the transfer eigenvalue problem, respectively, increases the chance of catching all relevant eigenfunctions, however, it may result in a larger coarse space dimension than necessary.

The case of Ω_e^{2h} shows that the tolerance has to be increased from 10^5 to 10^6 in order to omit those eigenmodes which result in a too large coarse space dimension; this is also reflected in the results in Table 1.

Furthermore, we observe that there is a significant amount of linearly dependent edge basis functions for the new coarse space; this results from the fact that we combine the constant function and eigenfunctions from the Dirichlet and transfer eigenvalue problem. Due to POD orthogonalization the total coarse space dimension is reduced by 12–15. Here, the resulting coarse space dimension of 57 is always optimal, which can be explained as follows: For each edge, we need at least one (constant) function, and in case of channels cutting the edge, at least as many functions as channels. This yields $12 + 3 \times 12 = 48$ edge functions. In addition to that, we obtain one function for each of the 9 vertices, resulting in a dimension of 57.

Finally, we report results for varying values of α_{\min} in Table 2. We observe that, for the classical GDSW coarse space, condition number and iteration count deteriorate; in particular, the condition number is in the order of the coefficient contrast. For the $X_{\text{VCDT-}l^2}$ coarse space, the results are robust and independent of α_{\min} .

8.2. Algebraic and non-algebraic variants of the transfer eigenvalue problem. It is remarkable that, as observed in subsection 8.1, both the $X_{\text{VCDT-}l^2}$ and $X_{\text{VCDT-}a}$ variants yield comparable results when investigating the eigenvalue problems in more detail. In Fig. 5, we plot the functions appearing in the eigenvalue problem. Even though the traces of the

α_{\min}	X_0	tol_{tr}	$\dim X_0$	κ	# its.
10^{-2}	X_{GDSW}	–	33 / 33	$2.7 \cdot 10^7$	142
	$X_{\text{VCDT-}l^2}$	10^4	57 / 93	7.3	25
1	X_{GDSW}	–	33 / 33	$2.7 \cdot 10^5$	118
	$X_{\text{VCDT-}l^2}$	10^4	57 / 93	7.2	25
10^2	X_{GDSW}	–	33 / 33	$2.7 \cdot 10^3$	95
	$X_{\text{VCDT-}l^2}$	10^4	57 / 69	8.5	25

TABLE 2. Numerical results for the coefficient function shown in Fig. 3 (left) with varying α_{\min} , 4×4 subdomains with $H/h = 10$, and $\alpha_{\max} = 10^6$ and $\alpha_{\min} = 1$ using the classical X_{GDSW} coarse space and the adaptive $X_{\text{VCDT-}l^2}$ coarse space for $\Omega_e = \Omega_e^{5h}$; see also Fig. 3 (left). We report the coarse space dimension (final dimension / dimension before POD orthogonalization), the estimated condition number, and the iteration count.

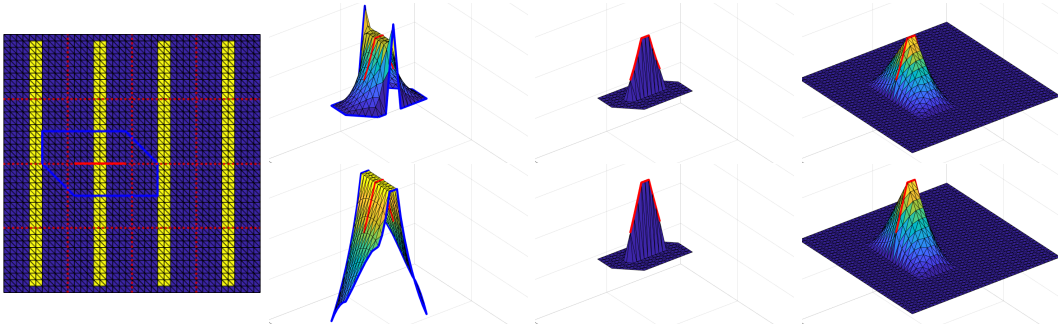


FIGURE 5. Simple coefficient distribution with one vertical channel cutting each horizontal edge (left/1st column); the discrete interior edge \tilde{e} and $\partial\Omega_e$ are plotted as solid red and blue lines, respectively. Visualization of the different functions arising in the transfer eigenvalue problem for $X_{\text{VCDT-}l^2}$ (top) and $X_{\text{VCDT-}a}$ (bottom): $H_{e \rightarrow \Omega_e}^{\partial\Omega_e} \varphi_e^{(i)}$ (2nd column), $E_{e \rightarrow \Omega_e} \varphi_e^{(i)}$ (3rd column), and $H_{\Gamma \rightarrow \Omega} (E_{e \rightarrow \Gamma} \varphi_e^{(i)})$ (4th column).

chosen eigenfunctions on $\partial\Omega_e$ (corresponding to the channel) differ significantly due to the different inner products, the trace on e is almost the same. Hence, the resulting coarse basis functions, which are computed by extending the edge values into the interior, span almost the same space.

8.3. Coarse space reduction by enlarging Ω_e . In subsection 8.1, we already observed the influence of the size of Ω_e on the spectra of the eigenvalue problems. Here, we discuss a second example, which is visualized in Fig. 3 (right), where the effect is even stronger and better interpretable.

It can be observed that a single edge function, and thus a coarse space of dimension 33, is sufficient for robustness for this example because there is only a single connected high coefficient component cutting each edge. Consequently, in the results in Table 3, even the classical GDSW coarse yields good results. This can only be detected by the eigenvalue problem if Ω_e is large enough to cover this whole high-coefficient component. If Ω_e is too small, the high coefficient component appears as either three, two, or one component cutting the edge for Ω_e^{2h} , Ω_e^{5h} , or Ω_e^H , respectively; cf. Fig. 3 (right). Also when using the two subdomains adjacent to the edge e as the domain for the energy minimizing extension, as in the default AGDSW approach, the component is detected as a whole.

X_0	Ω_{out}	tol_{tr}	$\dim X_0$	κ	# its.
X_{GDSW}	–	–	33 / 33	24.1	31
X_{AGDSW}	Ω_e^{2h}	–	57 / 57	7.1	24
	Ω_e^{5h}	–	45 / 45	12.6	26
	Ω_e^H	–	33 / 33	24.1	31
	–	–	33 / 33	24.1	31
$X_{\text{VCDT-}l^2}$	Ω_e^{2h}	10^6	57 / 69	7.1	24
	Ω_e^{5h}	10^5	45 / 57	17.1	33
	Ω_e^H	10^5	33 / 57	24.1	31

TABLE 3. Numerical results for the coefficient function shown in Fig. 3 (right), 4×4 subdomains with $H/h = 10$, and $\alpha_{\max} = 10^6$ and $\alpha_{\min} = 1$ using different coarse spaces; in case of the novel coarse spaces $X_{\text{VCDT-}*}$, we vary the size of Ω_e : two layers of finite elements (Ω_e^{2h}), five layers of finite elements (Ω_e^{5h}), or one layer of subdomains (Ω_e^H) around e ; see also Fig. 3 (right). We report the coarse space dimension (final dimension / dimension before POD orthogonalization), the estimated condition number, and the iteration count. Non-default tolerances tol_{tr} are marked in **bold face**.

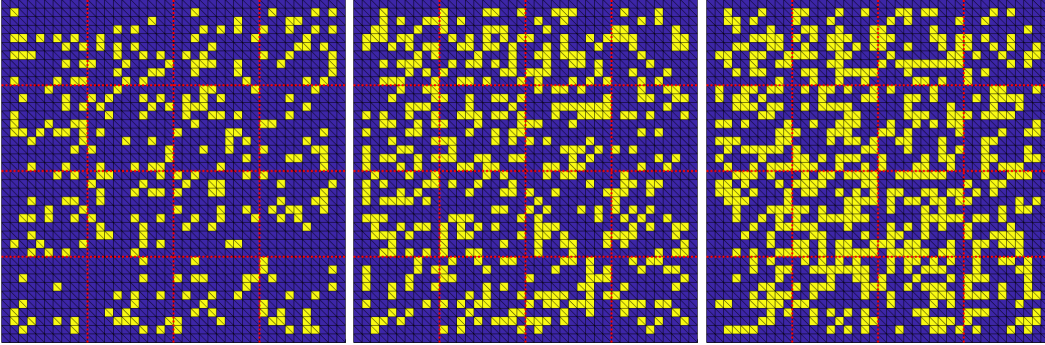


FIGURE 6. Exemplary random heterogeneous coefficient functions with 20 % (left), 30 % (middle), and 40 % (right) elements with high coefficient on a 4×4 subdomains with $H/h = 10$: the domain decomposition interface is depicted as dashed red lines, the elements with $\alpha = \alpha_{\max}$ are colored yellow, and the elements with $\alpha = \alpha_{\min}$ are colored dark blue.

This is also reflected clearly in the numerical results in Table 3. There are 12 edges cut by such a high-coefficient component. While increasing the size of Ω_e from Ω_e^{2h} to Ω_e^{5h} or Ω_e^H the coarse space dimension reduces by 12 or 24, respectively. The same behavior can be observed for AGDSW, when using Ω_e^{2h} , Ω_e^{5h} , and Ω_e^H as the extension domain. This effect has already been reported for similar cases in [27, 29].

8.4. Random coefficient distributions. In order to validate the theory and show robustness of our fully algebraic approach ($X_{\text{VCDT-}l^2}$ coarse space) for general coefficient distributions, we test it on randomly distributed binary coefficient distributions; examples for coefficient distributions with 20 %, 30 %, and 40 % elements with high coefficients are shown in Fig. 6.

The results are listed in Table 4, and we can draw several conclusions from those results: First, we generally obtain good convergence for our fully algebraic approach for different ratios of high coefficient elements and sizes of Ω_e . As we already observed before, enlarging Ω_e reduces the coarse space dimension, which is much more pronounced for larger ratios of

α_{\max}	Ω_{out}	tol_{tr}	$\dim X_0$	κ	# its.
20 %	Ω_e^{2h}	10^5	85.7 (105) / 128.5 (150)	12.1 (36.0)	30.1 (36)
	Ω_e^{5h}	10^5	62.6 (77) / 127.3 (158)	9.1 (27.9)	27.8 (32)
	Ω_e^H	10^5	62.4 (74) / 122.3 (142)	8.6 (11.6)	27.5 (31)
30 %	Ω_e^{2h}	10^5	121.6 (143) / 154.8 (176)	20.6 (86.3)	30.0 (41)
	Ω_e^{5h}	10^5	70.6 (81) / 122.7 (143)	10.6 (25.5)	27.4 (34)
	Ω_e^H	10^5	62.9 (74) / 122.4 (143)	13.3 (38.4)	27.6 (37)
40 %	Ω_e^{2h}	10^7	79.9 (87) / 81.2 (88)	$1.1 \cdot 10^4$ ($9.6 \cdot 10^4$)	51.4 (105)
		10^6	119.0 (133) / 125.5 (136)	223.9 (1879.4)	34.6 (59)
		10^5	155.1 (172) / 180.7 (200)	17.2 (296.0)	25.5 (33)
		10^4	162.3 (179) / 190.9 (210)	6.7 (29.4)	21.7 (26)
	Ω_e^{5h}	10^5	81.3 (94) / 112.3 (126)	11.5 (40.6)	27.3 (34)
		10^5	59.0 (68) / 95.2 (116)	23.3 (76.9)	32.9 (44)

TABLE 4. Numerical results for randomly distributed coefficient function as shown in Fig. 6 with 20 %, 30 %, and 40 % high coefficient elements for 4×4 subdomains with $H/h = 10$, and $\alpha_{\max} = 10^6$ and $\alpha_{\min} = 1$ using different coarse spaces; in case of the novel coarse spaces $X_{\text{VCDT-}*}$, we vary the size of Ω_e : two layers of finite elements (Ω_e^{2h}), five layers of finite elements (Ω_e^{5h}), or one layer of subdomains (Ω_e^H) around e ; see also Fig. 3; for the Ω_e^{2h} case, we vary the threshold tol_{tr} . We report the coarse space dimension (final dimension / dimension before POD orthogonalization), the estimated condition number, and the iteration count averaged over 100 runs (maximum number in parentheses). Non-default tolerances tol_{tr} are marked in **bold face**.

high coefficient elements; for instance, for 40 % of high coefficient elements, the coarse space dimension can be reduced from 155.1 to 59.0 on average, when keeping the tolerances fixed.

Of course, enlarging Ω_e also increases the computational work for setting up both eigenvalue problems. As an alternative, we consider the smallest $\Omega_e = \Omega_e^{2h}$ and vary the threshold for the transfer eigenvalue problem for the tolerance: when increasing tol_{tr} from 10^4 to 10^6 , the coarse space dimension reduced from 162.3 to 119.0. At the same time, the condition number and iteration count increase moderately: the maximum iteration count goes up from 34 to 44 and the maximum condition number from 29.4 to 1879.4. When increasing the tolerance further to 10^7 , we obtain an even smaller coarse space dimension of 79.9; however, the maximum condition number and iteration count deteriorate to $9.6 \cdot 10^4$ and 105, respectively. Obtaining robustness using the fully algebraic coarse space depends on an interplay of the hyper parameters of the method, such as the size of Ω_e and the tolerances; a full investigation is not possible here due to space limitations.

8.5. SPE10 model problem. Finally, we consider a coefficient function based on realistic data. In particular, we use heterogeneous coefficient functions α generated from parts of the 40th layer of the second data set from the 2001 SPE Comparative Solution Project benchmark [12], employing the pixel-wise norm of the permeabilities as the coefficient function. As can be observed in Table 5 (“*Original coefficient (without thresholding)*”), this example can be solved robustly using the classical GDSW coarse space, and no adaptive coarse space is needed. However, if we convert α into a binary coefficient function by setting all coefficients above 1.0 to $\alpha_{\max} = 10^6$ and all coefficients below 1.0 to $\alpha_{\min} = 1$, the classical GDSW coarse space is not robust anymore, resulting in a high condition number of $2.0 \cdot 10^5$.

As expected, the X_{AGDSW} and $X_{\text{VCDT-}l^2}$ adaptive coarse spaces yield robust results. For small sizes of Ω_e , the dimension of the $X_{\text{VCDT-}l^2}$ coarse space is quite high; for instance, the coarse space dimension is 362 for $\Omega_e = \Omega_e^{2h}$ (and $tol_{tr} = 10^5$). We observe that, the coarse space dimension reduces significantly when increasing tol_{tr} ; for $tol_{tr} = 10^7$, the dimension

X_0	Ω_{out}	tol_{tr}	$\dim X_0$	κ	# its.
Original coefficient (without thresholding)					
X_{GDSW}	–	–	85 / 85	20.6	42
Binary coefficient (with thresholding)					
X_{GDSW}	–	–	85 / 85	$2.0 \cdot 10^5$	57
X_{AGDSW}	–	–	93 / 93	19.3	38
$X_{\text{VCDT-}l^2}$		10^7	147 / 150	1859.0	40
	Ω_e^{2h}	10^6	262 / 273	122.8	37
		10^5	362 / 417	9.3	31
	Ω_e^{5h}	10^5	191 / 229	9.3	31
	Ω_e^H	10^5	147 / 176	9.6	31
X_{VCD}	Ω_e^{2h}	–	87 / 89	$2.0 \cdot 10^5$	57
	Ω_e^{5h}	–	90 / 92	19.4	39
	Ω_e^H	–	90 / 93	19.4	39

TABLE 5. Numerical results for the coefficient functions shown in Fig. 7 (with and without thresholding), 6×6 subdomains with $H/h = 10$ using different coarse spaces; in case of the novel coarse spaces $X_{\text{VCDT-}*}$, we vary the size of Ω_e : two layers of finite elements (Ω_e^{2h}), five layers of finite elements (Ω_e^{5h}), or one layer of subdomains (Ω_e^H) around e ; see also Fig. 3; for the Ω_e^{2h} case, we vary the threshold tol_{tr} . We report the coarse space dimension (final dimension / dimension before POD orthogonalization), the estimated condition number, and the iteration count. Non-default tolerances are marked in **bold face**.

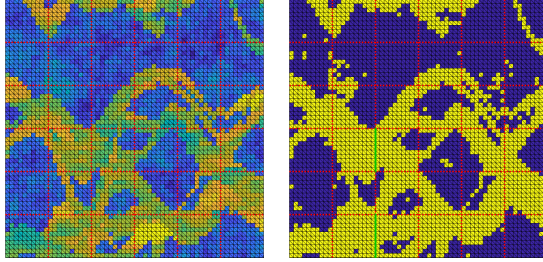


FIGURE 7. Heterogeneous coefficient functions on 6×6 subdomains with $H/h = 10$; the domain decomposition interface is depicted as dashed red lines. **Left:** Coefficient values are between $\alpha_{\max} = 2.9 \cdot 10^4$ (yellow) and $\alpha_{\min} = 5.8 \cdot 10^{-3}$ (dark blue). **Right:** Binary heterogeneous coefficient function created with a threshold of 1: every coefficient above 1 is mapped to $\alpha_{\max} = 10^6$, and every coefficient below 1 is mapped to $\alpha_{\min} = 1$.

is only 147. The same dimension is obtained for $\Omega_e = \Omega_e^H$. While enlarging Ω_e results in a better condition number and iteration count, it also increases the computational cost for setting up the eigenvalue problems. On the other hand, increasing tol_{tr} does not increase the computational cost; however, the condition number and iteration count grow moderately.

For this example, we also report results for the space X_{VCD} , where the transfer eigenvalue problem is completely neglected. While the condition number is contrast dependent for $\Omega_e = \Omega_e^{2h}$, which shows that the transfer eigenvalue problem is necessary in this case, we obtain good results for $\Omega_e = \Omega_e^{5h}$ and $\Omega_e = \Omega_e^H$, and the dimension of the coarse space is even lower than the dimension of X_{AGDSW} . Note that for oversampling domains where the coefficient function is high nearly everywhere, we conjecture a slower decay of the harmonic extensions of higher frequency modes on $\partial\Omega_e$. This results in a relatively large $X_{\text{VCD-}l^2}$ space on e ; this is the case, for example, for the green vertical edges in Fig. 7.

These results show that our fully algebraic approach is very robust, but further investigations of choosing the thresholds will be necessary to obtain the optimal coarse space dimension.

REFERENCES

- [1] E. AGULLO, L. GIRAUD, AND L. POIREL, *Robust preconditioners via generalized eigenproblems for hybrid sparse linear solvers*, SIAM J. Matrix Anal. Appl., 40 (2019), pp. 417–439.
- [2] H. AL DAAS AND L. GRIGORI, *A class of efficient locally constructed preconditioners based on coarse spaces*, SIAM J. Matrix Anal. Appl., 40 (2019), pp. 66–91.
- [3] H. AL DAAS AND P. JOLIVET, *A Robust Algebraic Multilevel Domain Decomposition Preconditioner For Sparse Symmetric Positive Definite Matrices*, arXiv:2109.05908, (2021).
- [4] H. AL DAAS, P. JOLIVET, AND T. REES, *Efficient Algebraic Two-Level Schwarz Preconditioner For Sparse Matrices*, arXiv:2201.02250, (2022).
- [5] I. BABUŠKA AND R. LIPTON, *Optimal local approximation spaces for generalized finite element methods with application to multiscale problems*, Multiscale Model. Simul., 9 (2011), pp. 373–406.
- [6] P. BASTIAN, R. SCHEICHL, L. SEELINGER, AND A. STREHLOW, *Multilevel spectral domain decomposition*, SIAM J. Sci. Comput., 0 (0), pp. S1–S26.
- [7] L. BEIRÃO DA VEIGA, L. F. PAVARINO, S. SCACCHI, O. B. WIDLUND, AND S. ZAMPINI, *Adaptive selection of primal constraints for isogeometric BDDC deluxe preconditioners*, SIAM J. Sci. Comput., 39 (2017), pp. A281–A302.
- [8] G. BERKOOZ, P. HOLMES, AND J. L. LUMLEY, *The proper orthogonal decomposition in the analysis of turbulent flows*, Annu. Rev. Fluid Mech., 25 (1993), pp. 539–575.
- [9] A. BUHR AND K. SMETANA, *Randomized Local Model Order Reduction*, SIAM J. Sci. Comput., 40 (2018), pp. A2120–A2151.
- [10] J. G. CALVO AND O. B. WIDLUND, *An adaptive choice of primal constraints for BDDC domain decomposition algorithms*, Electron. Trans. Numer. Anal., 45 (2016), pp. 524–544.
- [11] T. CHARTIER ET AL., *Spectral AMGe (ρ AMGe)*, SIAM J. Sci. Comput., 25 (2003), pp. 1–26.
- [12] M. A. CHRISTIE AND M. BLUNT, *Tenth SPE comparative solution project: A comparison of upscaling techniques*, SPE Reservoir Evaluation & Engineering, 4 (2001), pp. 308–317.
- [13] C. R. DOHRMANN, A. KLAWONN, AND O. B. WIDLUND, *Domain decomposition for less regular subdomains: overlapping Schwarz in two dimensions*, SIAM J. Numer. Anal., 46 (2008), pp. 2153–2168.
- [14] C. R. DOHRMANN, A. KLAWONN, AND O. B. WIDLUND, *A family of energy minimizing coarse spaces for overlapping Schwarz preconditioners*, in Domain decomposition methods in science and engineering XVII, vol. 60 of Lect. Notes Comput. Sci. Eng., Springer, Berlin, 2008, pp. 247–254.
- [15] V. DOLEAN, F. NATAF, R. SCHEICHL, AND N. SPILLANE, *Analysis of a two-level Schwarz method with coarse spaces based on local Dirichlet-to-Neumann maps*, Comput. Methods Appl. Math., 12 (2012), pp. 391–414.
- [16] M. DRYJA AND O. B. WIDLUND, *Domain decomposition algorithms with small overlap*, SIAM J. Sci. Comput., 15 (1994), pp. 604–620.
- [17] E. EIKELAND, L. MARCINKOWSKI, AND T. RAHMAN, *Overlapping Schwarz methods with adaptive coarse spaces for multiscale problems in 3D*, Numer. Math., 142 (2019), pp. 103–128.
- [18] J. GALVIS AND Y. EFENDIEV, *Domain decomposition preconditioners for multiscale flows in high-contrast media*, Multiscale Model. Simul., 8 (2010), pp. 1461–1483.
- [19] J. GALVIS AND Y. EFENDIEV, *Domain decomposition preconditioners for multiscale flows in high contrast media: reduced dimension coarse spaces*, Multiscale Model. Simul., 8 (2010), pp. 1621–1644.
- [20] M. J. GANDER, A. LONELAND, AND T. RAHMAN, *Analysis of a New Harmonically Enriched Multiscale Coarse Space for Domain Decomposition Methods*, arXiv:1512.05285, (2015).
- [21] S. GIPPERT, A. KLAWONN, AND O. RHEINBACH, *Analysis of FETI-DP and BDDC for Linear Elasticity in 3D with Almost Incompressible Components and Varying Coefficients Inside Subdomains*, SIAM J. Numer. Anal., 50 (2012), pp. 2208–2236.
- [22] G. H. GOLUB AND C. F. VAN LOAN, *Matrix computations*, Baltimore, MD: The Johns Hopkins University Press, 4th ed., 2013.
- [23] L. GOUARIN AND N. SPILLANE, *Fully algebraic domain decomposition preconditioners with adaptive spectral bounds*, arXiv:2106.10913, (2021).
- [24] I. GRAHAM, P. LECHNER, AND R. SCHEICHL, *Domain decomposition for multiscale PDEs*, Numer. Math., 106 (2007), pp. 589–626.

- [25] A. HEINLEIN, *Parallel Overlapping Schwarz Preconditioners and Multiscale Discretizations with Applications to Fluid-Structure Interaction and Highly Heterogeneous Problems*, PhD thesis, Universität zu Köln, June 2016.
- [26] A. HEINLEIN, C. HOCHMUTH, AND A. KLAWONN, *Fully algebraic two-level overlapping Schwarz preconditioners for elasticity problems*, in Numerical mathematics and advanced applications—ENUMATH 2019, vol. 139 of Lect. Notes Comput. Sci. Eng., Springer, Cham, 2021, pp. 531–539.
- [27] A. HEINLEIN, A. KLAWONN, J. KNEPPER, AND O. RHEINBACH, *An adaptive GDSW coarse space for two-level overlapping Schwarz methods in two dimensions*, in Domain Decomposition Methods in Science and Engineering XXIV, vol. 125 of Lect. Notes Comput. Sci. Eng., Springer, Cham, 2018, pp. 373–382.
- [28] A. HEINLEIN, A. KLAWONN, J. KNEPPER, AND O. RHEINBACH, *Multiscale coarse spaces for overlapping Schwarz methods based on the ACMS space in 2D*, Electron. Trans. Numer. Anal., 48 (2018), pp. 156–182.
- [29] A. HEINLEIN, A. KLAWONN, J. KNEPPER, AND O. RHEINBACH, *Adaptive GDSW coarse spaces for overlapping Schwarz methods in three dimensions*, SIAM J. Sci. Comput., 41 (2019), pp. A3045–A3072.
- [30] A. HEINLEIN, A. KLAWONN, J. KNEPPER, O. RHEINBACH, AND O. B. WIDLUND, *Adaptive GDSW coarse spaces of reduced dimension for overlapping Schwarz methods*, SIAM J. Sci. Comput., 44 (2022), pp. A1176–A1204.
- [31] A. HEINLEIN, A. KLAWONN, M. LANSER, AND J. WEBER, *A frugal FETI-DP and BDDC coarse space for heterogeneous problems*, Electron. Trans. Numer. Anal., 53 (2020), pp. 562–591.
- [32] A. HEINLEIN, A. KLAWONN, AND O. RHEINBACH, *A parallel implementation of a two-level overlapping Schwarz method with energy-minimizing coarse space based on Trilinos*, SIAM J. Sci. Comput., 38 (2016), pp. C713–C747.
- [33] G. KARYPIS, *A software package for partitioning unstructured graphs, partitioning meshes, and computing fill-reducing orderings of sparse matrices version 5.0*, 1998.
- [34] G. KARYPIS AND V. KUMAR, *A fast and high quality multilevel scheme for partitioning irregular graphs*, SIAM J. Sci. Comput., 20 (1998), pp. 359–392.
- [35] H. H. KIM, E. CHUNG, AND J. WANG, *BDDC and FETI-DP preconditioners with adaptive coarse spaces for three-dimensional elliptic problems with oscillatory and high contrast coefficients*, J. Comput. Phys., 349 (2017), pp. 191–214.
- [36] A. KLAWONN, M. KÜHN, AND O. RHEINBACH, *Adaptive coarse spaces for FETI-DP in three dimensions*, SIAM J. Sci. Comput., 38 (2016), pp. A2880–A2911.
- [37] A. KLAWONN, P. RADTKE, AND O. RHEINBACH, *FETI-DP methods with an adaptive coarse space*, SIAM J. Numer. Anal., 53 (2015), pp. 297–320.
- [38] A. KLAWONN, P. RADTKE, AND O. RHEINBACH, *A comparison of adaptive coarse spaces for iterative substructuring in two dimensions*, Electron. Trans. Numer. Anal., 45 (2016), pp. 75–106.
- [39] J. KNEPPER, *Adaptive Coarse Spaces for the Overlapping Schwarz Method and Multiscale Elliptic Problems*, phd thesis, University of Cologne, Cologne, Germany, 2022.
- [40] R. KORNUBER, D. PETERSEIM, AND H. YSERENTANT, *An analysis of a class of variational multiscale methods based on subspace decomposition*, Math. Comp., 87 (2018), pp. 2765–2774.
- [41] R. KORNUBER AND H. YSERENTANT, *Numerical homogenization of elliptic multiscale problems by subspace decomposition*, Multiscale Model. Simul., 14 (2016), pp. 1017–1036.
- [42] C. MA, R. SCHEICHL, AND T. DODWELL, *Novel design and analysis of generalized finite element methods based on locally optimal spectral approximations*, SIAM J. Numer. Anal., 60 (2022), pp. 244–273.
- [43] A. MÅLQVIST AND D. PETERSEIM, *Localization of elliptic multiscale problems*, Math. Comp., 83 (2014), pp. 2583–2603.
- [44] J. MANDEL AND B. SOUSEDÍK, *Adaptive selection of face coarse degrees of freedom in the BDDC and the FETI-DP iterative substructuring methods*, Comput. Methods Appl. Mech. Engrg., 196 (2007), pp. 1389–1399.
- [45] D.-S. OH, O. B. WIDLUND, S. ZAMPINI, AND C. R. DOHRMANN, *BDDC Algorithms with deluxe scaling and adaptive selection of primal constraints for Raviart-Thomas vector fields*, Math. Comp., 87 (2018), pp. 659–692.
- [46] H. OWHADI, *Multigrid with rough coefficients and multiresolution operator decomposition from hierarchical information games*, SIAM Rev., 59 (2017), pp. 99–149.
- [47] H. OWHADI AND L. ZHANG, *Localized bases for finite-dimensional homogenization approximations with nonseparated scales and high contrast*, Multiscale Model. Simul., 9 (2011), pp. 1373–1398.
- [48] H. OWHADI, L. ZHANG, AND L. BERLYAND, *Polyharmonic homogenization, rough polyharmonic splines and sparse super-localization*, ESAIM Math. Model. Numer. Anal., 48 (2014), pp. 517–552.
- [49] C. PECHSTEIN AND C. R. DOHRMANN, *A unified framework for adaptive BDDC*, Electron. Trans. Numer. Anal., 46 (2017), pp. 273–336.
- [50] A. PINKUS, *n-widths in approximation theory*, vol. 7, Springer-Verlag, Berlin, 1985.

- [51] A. QUARTERONI AND A. VALLI, *Domain decomposition methods for partial differential equations*, Numerical Mathematics and Scientific Computation, The Clarendon Press, Oxford University Press, New York, 1999.
- [52] J. W. RUGE AND K. STÜBEN, *Algebraic multigrid*, in Multigrid methods, SIAM, 1987, pp. 73–130.
- [53] J. SCHLEUSS AND K. SMETANA, *Optimal local approximation spaces for parabolic problems*, Multiscale Model. Simul., 20 (2022), pp. 551–582.
- [54] L. SIROVICH, *Turbulence and the dynamics of coherent structures. I. Coherent structures*, Quart. Appl. Math., 45 (1987), pp. 561–571.
- [55] K. SMETANA AND A. T. PATERA, *Optimal local approximation spaces for component-based static condensation procedures*, SIAM J. Sci. Comput., 38 (2016), pp. A3318–A3356.
- [56] N. SPILLANE, *An abstract theory of domain decomposition methods with coarse spaces of the geneo family*, arXiv preprint arXiv:2104.00280, (2021).
- [57] N. SPILLANE, *Toward a new fully algebraic preconditioner for symmetric positive definite problems*, tech. report, 2021.
- [58] N. SPILLANE, V. DOLEAN, P. HAURET, F. NATAF, C. PECHSTEIN, AND R. SCHEICHL, *Abstract robust coarse spaces for systems of PDEs via generalized eigenproblems in the overlaps*, Numer. Math., 126 (2014), pp. 741–770.
- [59] N. SPILLANE AND D. J. RIXEN, *Automatic spectral coarse spaces for robust finite element tearing and interconnecting and balanced domain decomposition algorithms*, Internat. J. Numer. Methods Engrg., 95 (2013), pp. 953–990.
- [60] A. TOSELLI AND O. WIDLUND, *Domain decomposition methods—algorithms and theory*, vol. 34 of Springer Series in Computational Mathematics, Springer-Verlag, Berlin, 2005.
- [61] S. ZAMPINI, *PCBDDC: a class of robust dual-primal methods in PETSc*, SIAM J. Sci. Comput., 38 (2016), pp. S282–S306.

DELFT INSTITUTE OF APPLIED MATHEMATICS, DELFT UNIVERSITY OF TECHNOLOGY, THE NETHERLANDS.
A.HEINLEIN@TUDELFT.NL

DEPARTMENT OF MATHEMATICAL SCIENCES, STEVENS INSTITUTE OF TECHNOLOGY, 1 CASTLE POINT TERRACE, HOBOKEN, NJ 07030, UNITED STATES OF AMERICA. KSMETANA@STEVENS.EDU